CHAPTER 6

RESULTS AND DISCUSSION

6.1 THERMAL STUDIES

6.1.1 Tube and muffle furnace

Table 6.1 shows the effect of various reaction parameters on the CaS yield during the thermal conversion of gypsum to CaS.

Effect of time. Experiment 1 (Table 6.1) showed that good conversion yields (> 96%) were achieved at a reaction time of 20 min. At a reaction time of 5 min, the yield was only 45%.

Effect of temperature. Experiment 2 (Table 6.1) indicated a marked improvement in the yield of the reduced mass as temperature was raised from 900 °C to 1 100 °C. The results showed further that for a carbon: gypsum mole ratio of 3:1 and a reaction time of 20 min, the conversion percentage increased from 15% at 900 °C to 96% at 1 100 °C . This could be due to the high activation energy required for the reduction of calcium sulphate to calcium sulphide. Saeed (1983) showed that the reaction between carbon and $CaSO_4$ to CaS takes place between 750 °C and 1 100 °C.

Effect of carbon: gypsum mole ratio. Experiment 3 (Table 6.1) showed that when no carbon was added, no CaS was formed. The addition of carbon to gypsum at a 1:1 mole ratio showed that only 20% of gypsum was converted to CaS. The conversion results further showed that CaO formation is favoured by a carbon: gypsum mole ratio of 1:1. Gypsum to CaO conversion of 38% was obtained. However, increasing the ratio of carbon to 2 and 3 moles to a given 1 mole of gypsum showed high conversions of gypsum to calcium sulphide (90 and 96%, respectively). The above results indicated that a reducing agent is needed for the thermal reduction of gypsum to CaS. The

high percentage conversion for a 1:2 molar ratio of gypsum to carbon corresponds to the stoichiometric amounts for the reaction of gypsum and carbon as indicated by reaction 83 (Reddy, *et al.,* 1967)

$$CaSO_4(s) + 2C(s) \rightarrow CaS(s) + 2CO_2(s) \quad (83)$$

Effect of particle size. Experiment 4 (Table 6.1) showed that the formation of calcium sulphide, is dependent upon the particle size of gypsum. When the gypsum particle size was 380 µm, the gypsum to CaS conversion was 80%. Increasing the particle size to 1 250 µm resulted in a decrease in the conversion. The improved yield of CaS afforded by 380 µm gypsum can be ascribed to the higher surface areas offered by the smaller particle size.

Effect of different reducing agents. Experiment 5 (Table 6.1) showed that the use of activated carbon as a reducing agent did not show a significantly increased yield of CaS when compared to coal. The use of activated carbon yielded 85% conversion, while coal yielded 81% conversion. The improved yield using Duff coal could be due to the volatiles contained in the coal. From these findings, it is recommended that coal be used as the reducing agent for a full scale plant. Duff coal is cheaper and readily available as compared to activated carbon.

Effect of different gypsum compounds. Experiment 6 (Table 6.1) showed that 91% of gypsum was converted to CaS when pure gypsum was used. The lower conversion percentages (76% and 81%) obtained when Anglo gypsum and Foskor gypsum were reduced to CaS can be ascribed to the impurities contained in the two gypsum compounds.

Effect of furnace type. Experiment 7 (Table 6.1) showed that the tube furnace (76%) is more efficient in converting gypsum to CaS than the muffle furnace (70%). The presence of oxygen in the muffle furnace resulted in the formation of several oxygen containing compounds such as $MgAl_2O_4$ and $Ca_2Al_2SiO_7$. However the tube furnace purged with nitrogen does not favour production of oxygen containing compounds.

Table 6.1 XRD analysis results for the thermal reduction of gypsum to CaS

Exp No.	Parameter	Value	Type of furnace	Type of gypsum	$CaSO_4$ %	CaS %	CaO %	MgO %	$Ca_2Al_2SiO_7$	$MgAl_2O_4$	$Ca_5(PO_4)_3OH$
1	Time (min)	5	Tube	Pure	49	45	7	0	0	0	0
		20			0	96	4	0	0	0	0
		60			0	93	5	0	0	0	0
2	Temperature (°C)	900	Tube	Pure	84	15	1	0	0	0	0
		1000			8	88	4	0	0	0	0
		1100			0	96	4	0	0	0	0
3	$C/CaSO_4$ mole ratio	0	Tube	Pure	100	0	0	0	0	0	0
		0.25			93	0	7	0	0	0	0
		0.5			74	0	25	0	0	0	0
		1			48	13	38	0	0	0	0
		2			2	90	8	0	0	0	0
		3			0	96	4	0	0	0	0
4	Particle size of Gypsum (µm)	380	Tube	Foskor	0	80	15	0	0	0	0
		630			22	56	18	0	0	0	0
		1250			86	1	12	0	0	0	0
5	Reducing agent	Coal	Tube	Foskor	8	81	5	0	0	0	3
		Activated carbon			7	85	4	0	0	0	2
6	Gypsum compounds	Pure	Tube	Pure	4	91	4	0	0	0	0
		Anglo		Anglo	8	76	7	7	0	0	0
		Foskor		Foskor	7	81	6	0	0	0	2
7	Furnace type	Tube	Tube	Anglo	8	76	6	8	0	0	0
		Muffle	Muffle		0	70	2	6	5	3	0

The following parameters were kept constant (in the above experiments) unless otherwise stated: temperature = 1100 °C, time = 20 min, mole ratio (carbon:gypsum) = 3: 1, gypsum amount = 5g and activated carbon was used as a reducing agent for experiment 1 to 4. For experiment 6 and 7, duff coal was used as a reducing agent.

6.1.2 Thermogravimetric analysis

The following thermogravimetric analysis were conducted when activated carbon/duff coal and pure/Anglo/Foskor gypsum were heated in nitrogen using a heating rate of 10 °C/min and a carbon/coal to gypsum ratio of 3:1 (unless otherwise stated).

6.1.2.1 Temperature study for the reaction between activated carbon and pure gypsum

Figure 6.1 shows the resultantthermogravimetric curve obtained when activated carbon and pure gypsum were heated to 1260 °C at a rate of 10 °C/min.

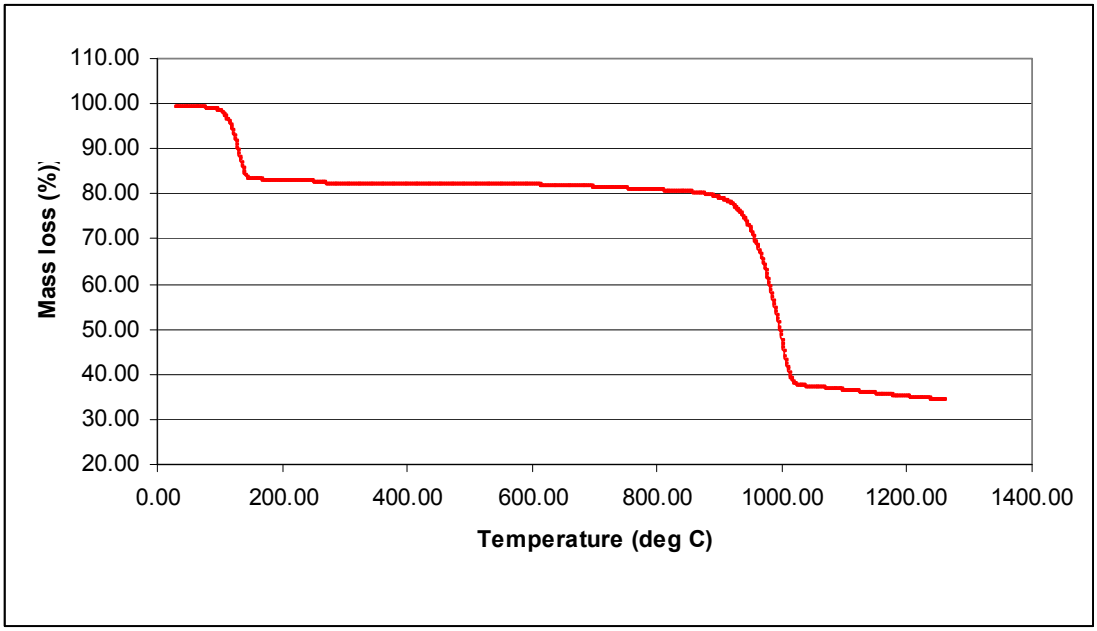

Figure 6.1 Thermogravimetric curve for the reaction between activated carbon and pure $CaSO_4.2H_2O$ at a heating rate of 10 °C/min

The effect recorded in the temperature range 80-180 °C was attributed to the loss of water of crystallisation from $CaSO_4.2H_2O$ to form $CaSO_4$ (reaction 84), (Popescu *et al.,* 1985).

$$CaSO_4.2H_2O\ (s) \rightarrow CaSO_4\ (s) + 2H_2O\ (g) \qquad (84)$$

The small mass loss between 600 °C and 850 °C was ascribed to the oxidation of carbon to carbon dioxide or carbon monoxide (reactions 85 and 86).

$$C\,(s) + O_2\,(g) \rightarrow CO_2\,(g) \quad (85)$$

$$2C\,(s) + O_2\,(g) \rightarrow 2CO\,(g) \quad (86)$$

The mass loss between 900 °C and 1 050 °C was due to the reduction of $CaSO_4$ to CaS with carbon (reaction 87). This finding confirmed the XRD results in Section 6.1 (Effect of temperature) which showed the presence of CaS between 900 °C and 1100 °C.

$$CaSO_4\,(s) + 2C\,(s) \rightarrow CaS\,(s) + 2CO_2\,(g) \quad (87)$$

Van der Merwe *et al*., (1999) showed that the descending thermogravimetric curve above 1 000 °C was due to the decomposition of the $CaSO_4$ to CaO (reaction 88)

$$CaSO_4\,(s) \rightarrow CaO\,(s) + SO_3\,(g) \quad (88)$$

6.1.2.2 Effect of carbon to gypsum mole ratio

Table 6.2 Thermogravimetric results for different mole ratios between activated carbon and pure $CaSO_4.2H_2O$

Mole ratio between carbon and gypsum (Carbon:Gypsum)	T_{min} (ºC)	T_{max} (ºC)	% mass loss	Total % mass loss
0.25:1	25	200	20.5	22.7
	200	800	2.1	
	800	1100	0.12	
0.5:1	25	200	20.6	23.3
	200	800	2.5	
	800	1100	0.17	
1:1	25	200	18.7	43.0
	200	800	5.7	
	800	1100	18.6	
3:1	25	200	17.9	60
	200	800	5.6	
	800	1100	36.2	

The results in Table 6.2 show the effect of different mole ratios of carbon to pure $CaSO_4.2H_2O$ at a heating rate of 10 °C/min. The amount of carbon was varied from 0.09 g to 1.04 g (0.25 mole to 3 mole) while that of gypsum was kept constant at 5 g. From the results in Table 6.2, it was seen that when the ratio between carbon and gypsum was 0.25:1, the mass loss was 23%. However, increasing the ratio of carbon to gypsum to 3:1 resulted in an increase in gypsum mass loss (60%). The finding emphasised the importance of adding a sufficient excess of reducing agent to effect the decomposition of calcium sulphate to CaS.

6.1.2.3 Effect of gypsum compounds and reducing agents

Table 6.3, Experiment 1 shows thermogravimetric results obtained for the comparison between three gypsum compounds from different sources using activated carbon as a reducing agent. The results showed that lower mass losses were obtained for Anglo and Foskor gypsum. This finding can also be ascribed to the constituent impurities as explained in Section 6.1.1. The mass loss of 44.8% in the case of pure gypsum, compared well with the theoretical mass loss for the reaction of pure $CaSO_4$ with carbon which is 44.9%.

From Experiment 2, it was seen that the use of coal as reducing agent results in lower mass losses with the three gypsum types. The carbon content of the Duff coal is 68.7% compared to the activated carbon which is 98.7%. This did not lower the conversion as much as expected. However, comparing the cost efficiency, the use of coal as a reducing agent in a full scale plant is recommended as discussed in Section 6.1

Table 6.3 Thermogravimetric results for the reaction between different gypsum compounds and reducing agents

Experiment number	Gypsum Source	Reducing agent	T_{min} (°C)	T_{max} (°C)	% mass loss
1	Pure Foskor Anglo	Activated carbon	650	1100	44.8 41.8 38.7
2	Pure Foskor Anglo	Duff coal	650	1100	38.5 32.9 30.5

6.1.3 Kinetic analysis

The kinetic analysis done on the thermogravimetric data obtained for the reaction between carbon monoxide and pure gypsum as well as the reaction between carbon and gypsum from three different sources (pure, Anglo and Foskor) is described in this section. Heating rates between 1 °C/min and 10 °C/min were utilised to calculate the activation energy values at different degrees of conversion (α) using the isoconversional method. The method provides a model free approximation of the activation energy, by using multiple scan analysis and is described by Ozawa (1965) and Flynn and Wall (1966).

The graphs represent the results of (1-α) (α is the degree of conversion) plotted against temperature for different heating rates, logarithm of heating rate vs reciprocal absolute temperature (log β vs. 1/T) at different degrees of conversion and the dependency of activation energy on the degree of conversion for each reaction mixture.

6.1.3.1 Reaction between carbon monoxide and pure gypsum

Six different heating rates between 1 °C/min and 10 °C/min were used to get the model free estimation of the activation energy of the reaction between carbon monoxide and pure gypsum (Figures 6.2-6.4). Figure 6.2 depicts the graph of (1 - α) versus temperature for different heating rates.

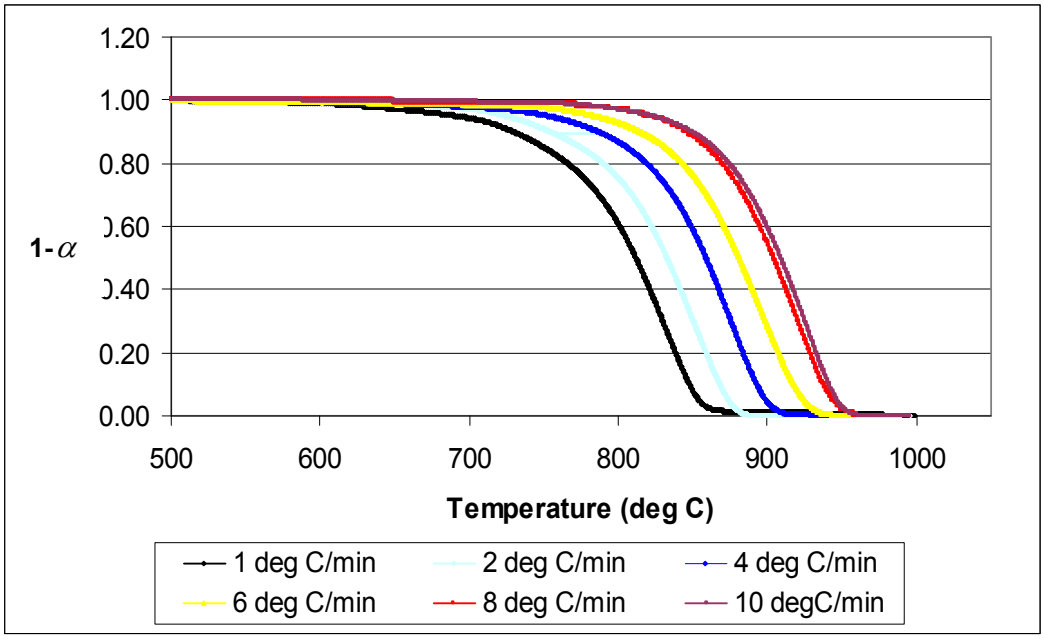

Figure 6.2 (1-α) versus temperature for six heating rates for the reaction between carbon monoxide and pure gypsum

The corresponding temperatures at a constant α at several heating rates were determined from degree of conversion versus temperature thermograms (Figure 6.2). The procedure was repeated at other values of the degree of conversion, thus testing the constancy of activation energy with respect to the degree of conversion and temperature. The graphs in Figure 6.3 show the plots made for logarithm of heating rate vs. reciprocal absolute temperature.

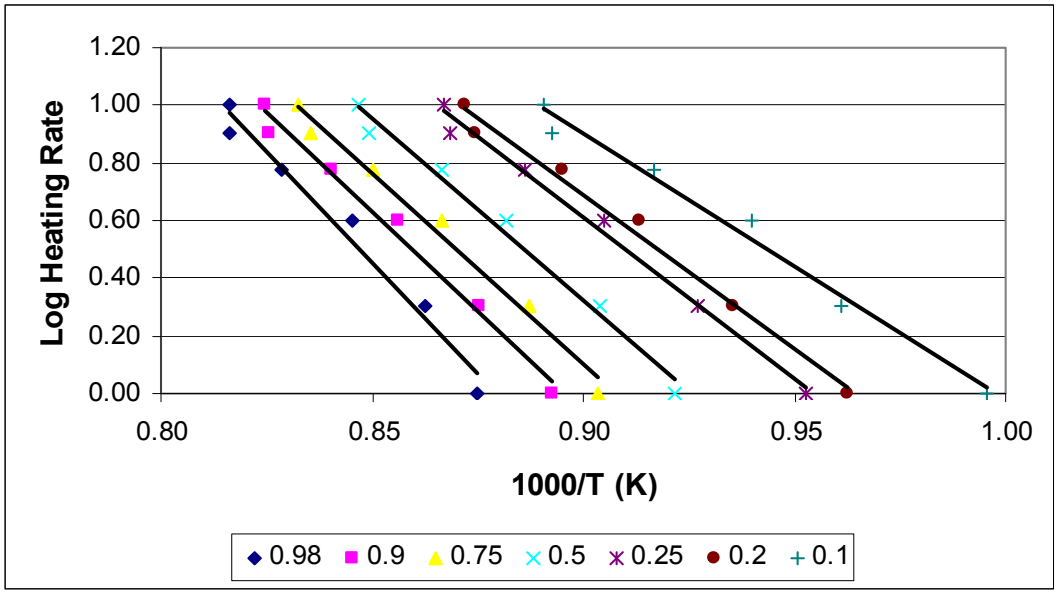

Figure 6.3 Logarithm of heating rate vs. reciprocal absolute temperature for the reaction between carbon monoxide and pure gypsum

For α equal to a constant, the plots of log β versus 1/T (Figure 6.3) were straight lines whose slopes give the activation energy at different degrees of conversion calculated from Equation 89. Figure 6.4 shows the dependency of activation energy on the degree of conversion.

$$E = -4.35 \frac{d \log \beta}{d \frac{1}{T}} \qquad (89)$$

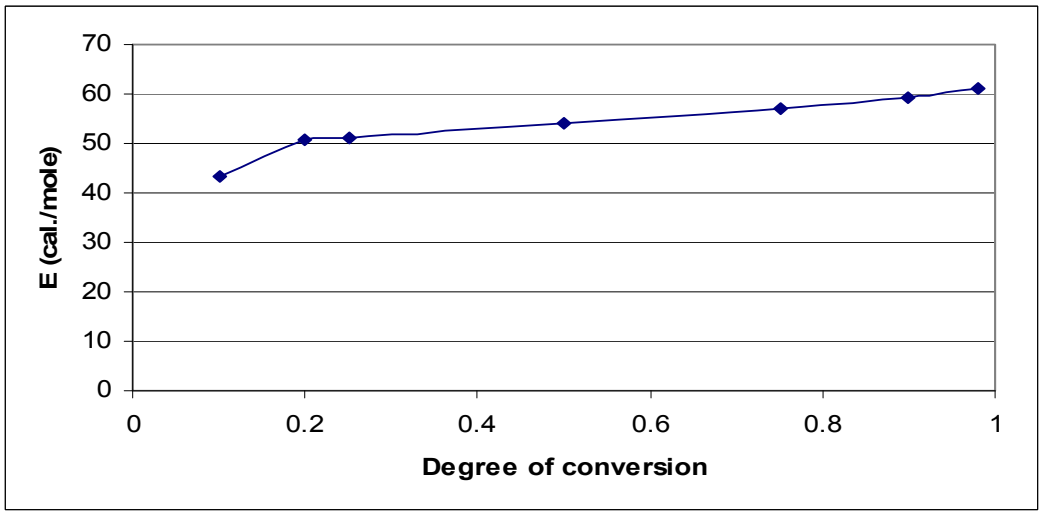

Figure 6.4 Dependency of the activation energy on the degree of conversion for the reaction between carbon monoxide and pure gypsum

6.1.3.2 Reaction between activated carbon and pure gypsum

Figures 6.5-6.7 show the temperature plotted against (1-α) for different heating rates (2, 4, 6, 8 and 10 °C/min); logarithm of heating rate vs reciprocal absolute temperature (log β vs. 1/T) at different degree of conversion, and the dependency of activation energy on the degree of conversion for the reaction between activated carbon and pure gypsum, respectively. The same procedures as indicated in 6.1.3.1 were followed.

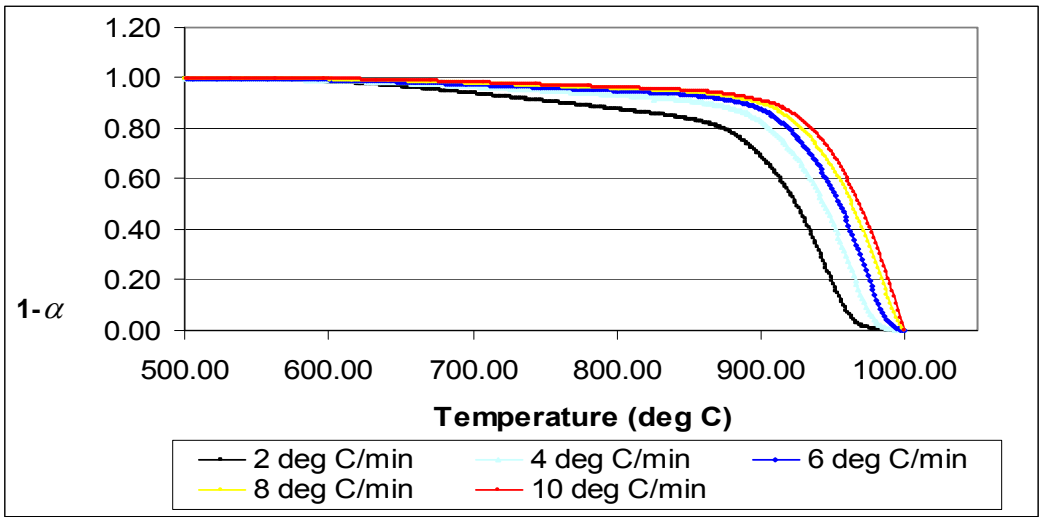

Figure 6.5 (1-α) versus temperature for five heating rates for the reaction between activated carbon and pure gypsum

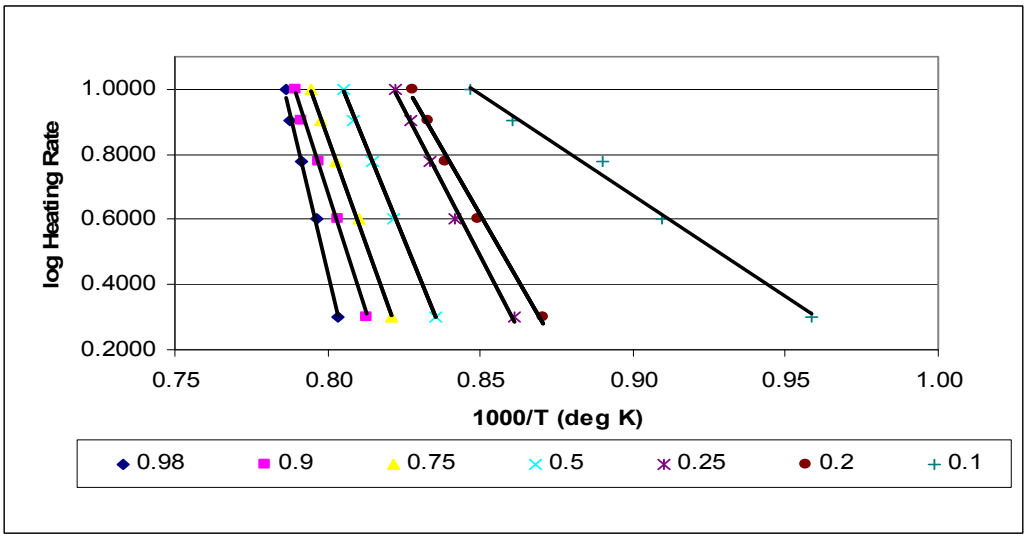

Figure 6.6 Logarithm of heating rate vs. reciprocal absolute temperature for the reaction between activated carbon and pure gypsum

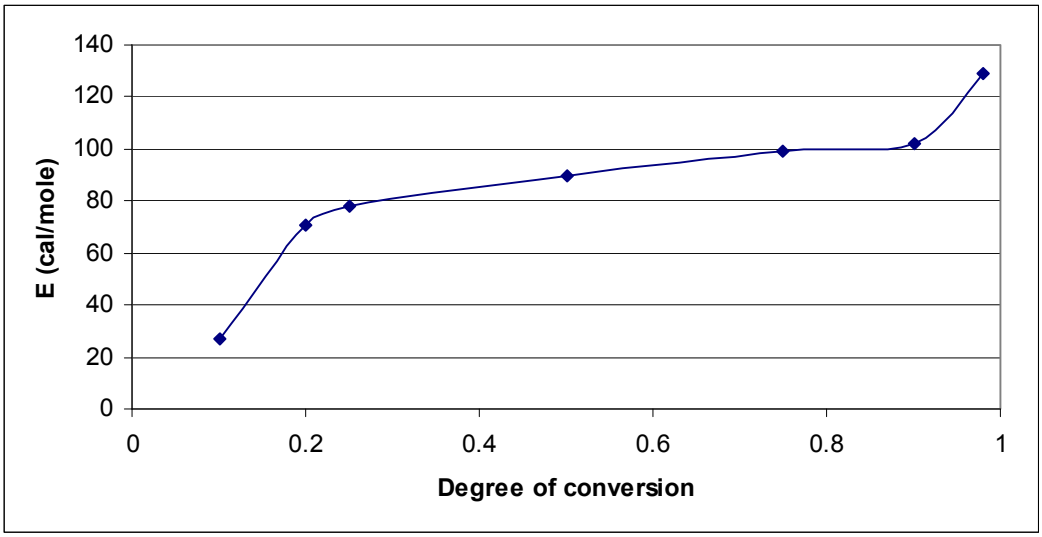

Figure 6.7 Dependency of the activation energy on the degree of conversion for the reaction between activated carbon and pure gypsum

6.1.3.3 Reaction between activated carbon and Foskor gypsum

The kinetic analysis done on the results obtained from the reaction between activated carbon and Foskor gypsum are shown in Figures 6.8-6.10.

The figures represent the temperature plotted against the (1-α) for different heating rates (2, 4, 6, 8 and 10 °C/min); logarithm of heating rate vs reciprocal absolute temperature (log β vs. 1/T) at different degrees of conversion, and the dependency of activation energy on the degree of conversion for the reaction between activated carbon and pure gypsum. The same procedures as indicated in 6.1.3.1 were followed.

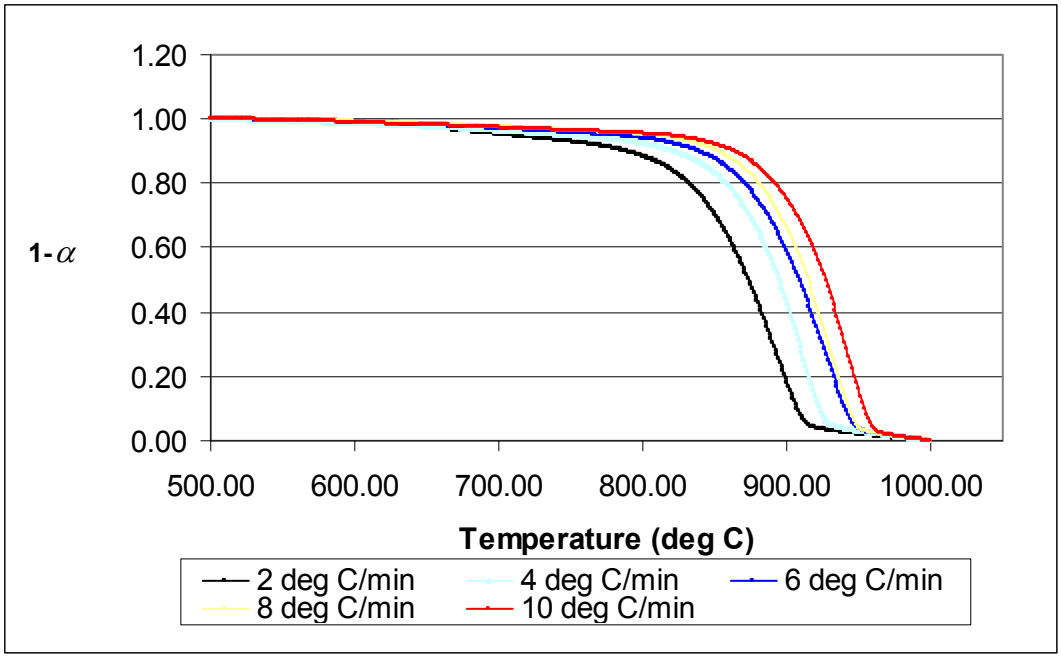

Figure 6.8 **(1-α) versus temperature for five heating rates for the reaction between activated carbon and Foskor gypsum**

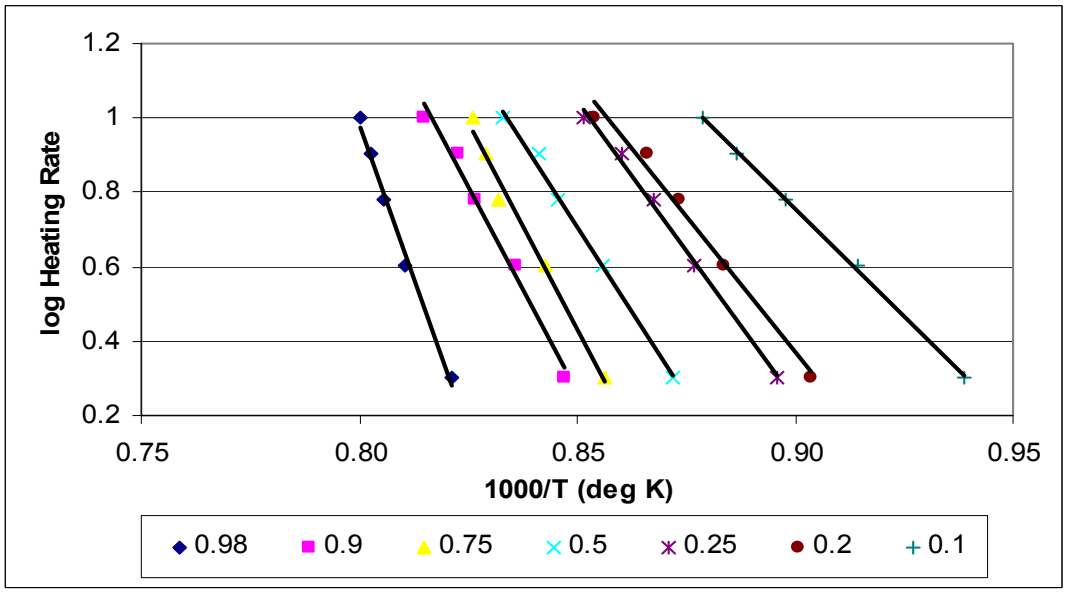

Figure 6.9 **Logarithm of heating rate versus reciprocal absolute temperature for the reaction between activated carbon and Foskor gypsum**

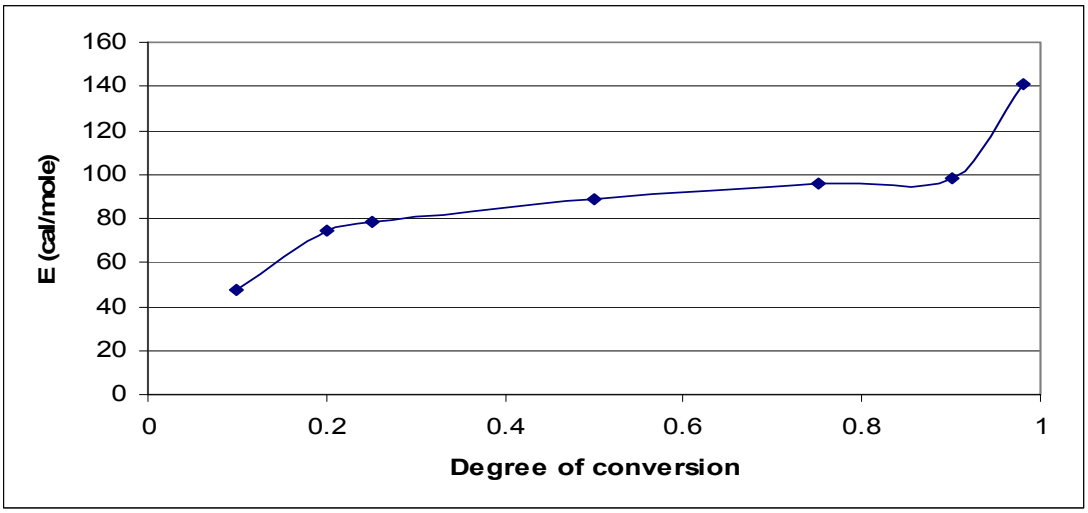

Figure 6.10 Dependency of the activation energy on the degree of conversion for the reaction between activated carbon and Foskor gypsum

6.1.3.4 Reaction between activated carbon and Anglo gypsum

Five heating rates (2, 4, 6, 8 and 10 °C/min) were utilized to obtain the activation energies for the reaction between activated carbon and Anglo gypsum. Figures 6.11-6.13 indicate temperature plotted against the (1 - α) for different heating rates (2, 4, 6, 8 and 10 °C/min); logarithm of heating rate vs reciprocal absolute temperature (log β vs. 1/T) at different degree of conversion, and the dependency of activation energy on the degree of conversion for the reaction between activated carbon and pure gypsum, respectively. The same procedures as indicated in 6.1.3.1 were followed.

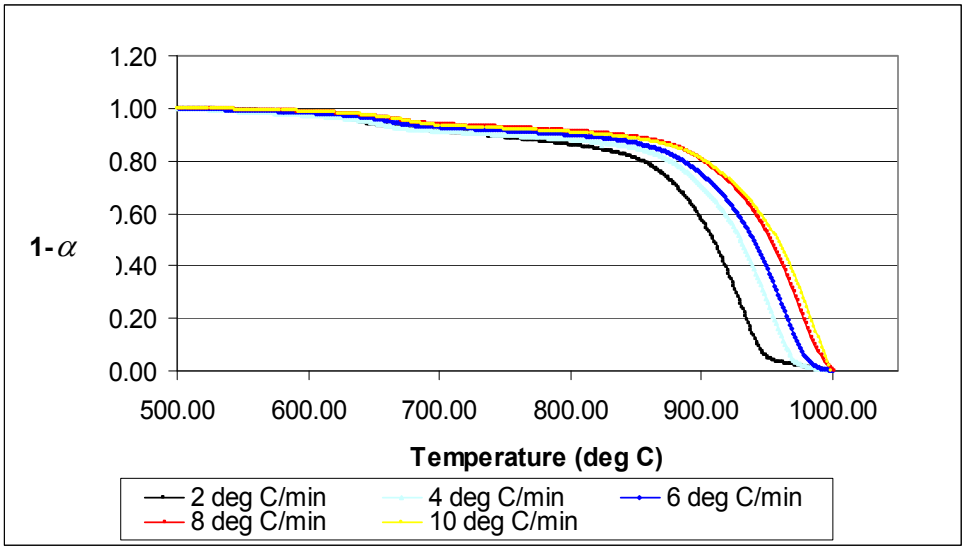

Figure 6.11 (1-α) versus temperature for six heating rates for the reaction between activated carbon and Anglo gypsum

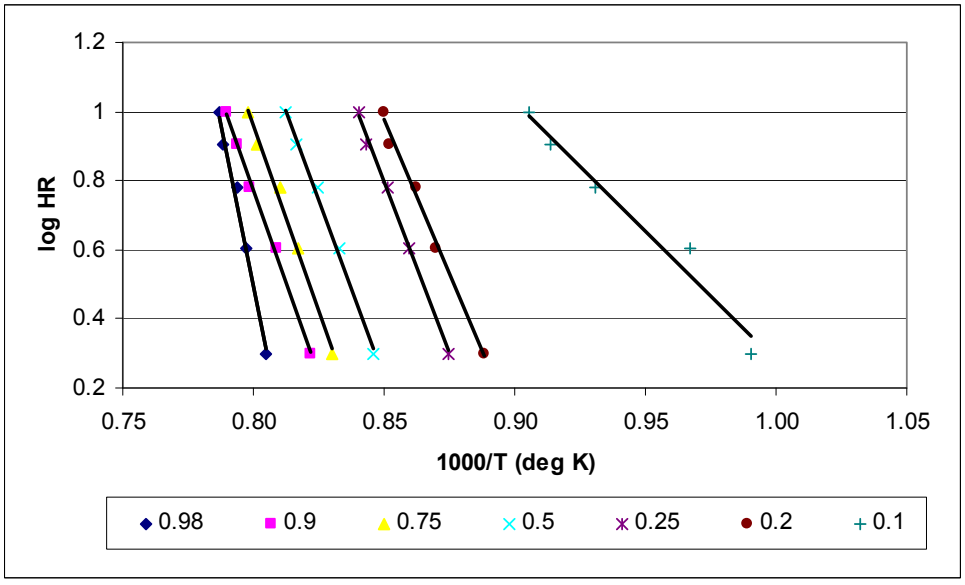

Figure 6.12 Logarithm of heating rate versus reciprocal absolute temperature for the reaction between activated carbon and Anglo gypsum

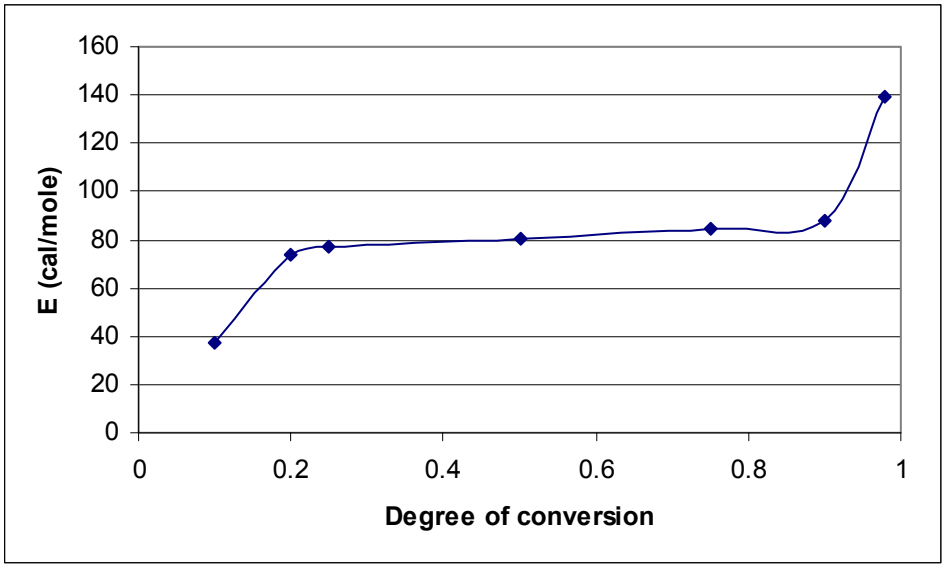

Figure 6.13 Dependency of the activation energy on the degree of conversion for the reaction between activated carbon and Anglo gypsum

Interpretation of the kinetic data.

Figures 6.2, 6.5, 6.8 and 6.11, representing the results for the degree of conversion plotted against temperature for the three gypsum types (pure, Anglo and Foskor) and the two reducing agents (activated carbon and Duff coal) at different heating rates showed that an increase in the heating rates from 1 to 10 °C/min, gave smooth curves.

Dowdy (1987) indicated that if the calculated activation energy for a certain reaction is the same for different degrees of conversion, it can be concluded that the reaction is a single step reaction. However, if the activation energy changes for different degrees of conversion, then the reaction is complex.

Applying Dowdy's conclusions about change in activation energy in Figures 6.4, 6.7, 6.10 and 6.13, representing the dependency of activation energy on the degree of conversion, it was concluded that the process under study, the thermal decomposition of gypsum in the presence of carbon/carbon monoxide, is complex.

Vyazovkin and Lesnikovich (1990) proposed a method for detailing the types of complex processes. They indicated that decreasing dependencies of activation energy on the degree of conversion show complex processes with a change in the limiting stage, e.g. processes containing a reversible intermediate stage or those with a change over from a kinetic to a diffusion controlled regime. Increasing dependencies of activation energy on the degree of conversion are characteristics of processes involving several parallel, competing reactions.

They further showed that by analysing the shape of the activation energy versus the degree of conversion curve, it may be possible to distinguish between complex processes incorporating parallel competing and parallel independent reactions. With parallel independent reactions a plateau shape is observed at the initial and final stages of conversion. Therefore, an S-shape characteristic curve is observed with parallel independent reactions (Vyazovkin *et al.*, 1992). In the case of parallel competing reactions, no S-shape characteristic curves are observed.

The above characteristics for detailing the types of complex processes were applied to the results obtained for the reaction between carbon monoxide/activated carbon and the different gypsum types (Figure 6.4, 6.7, 6.10 and 6.13). It was concluded that a complex of parallel competing reactions take place in the present study. This conclusion was supported by the following findings:

1) An increasing dependency of activation energy on the degree of conversion was observed from the four different Figures (6.4, 6.7, 6.10 and 6.13)
2) The increase in activation energy at the initial stage of the transformation (up to α=0.2) did not show a plateau and makes it possible to distinguish parallel competing reactions from a process incorporating parallel independent reactions.

Between the conversion degrees of 0.2 and 0.75, the absence of the activation energy dependency on the degree of conversion (plateau) was observed. The plateau shape indicates that there is no change in the limiting step. Possible reasons for no change in the dependency of activation energy on the degree of conversion could be due to different influences of the diffusion of gaseous products.

The figures further showed that the activation energies for the reaction between Anglo and Foskor gypsum with activated carbon were higher as compared to the activation energies for pure gypsum. This can possibly be ascribed to the impurities in Foskor gypsum and Anglo gypsum, which cause interference owing to side reactions.

Since the solid–solid reactions ($CaSO_4$ and C, reaction 90) are inherently slow as compared to gas - solid reactions ($CaSO_4$ and CO, reaction 93), it was proposed that reaction 90 occurs via intermediate reaction products, CO and CO_2 (reactions 91, 92 and 93). Figure 6.14 shows how $\Delta G°$ (Gibbs free energy, which is the measure of the thermodynamic driving force that makes a reaction occur) changes with temperature, at atmospheric pressure, for reactions 91 and 92, (Gaskell, 1993).

$$CaSO_4\,(s) + 2C\,(s) \rightarrow CaS\,(s) + 2CO_2\,(g) \quad (90)$$

$$C\,(s) + O_2\,(g) \rightarrow CO_2\,(g) \quad (91)$$

$$2C\,(s) + O_2\,(g) \rightarrow 2CO\,(g) \quad (92)$$

$$2CO\,(g) + O_2\,(g) \rightarrow 2CO_2\,(g) \quad (93)$$

$$\text{Overall reaction: } CaSO_4\,(s) + 4CO\,(g) \rightarrow CaS\,(s) + CO_2\,(g) \quad (94)$$

Figure 6.14 showed that of the two possible reactions (reactions 91 and 92) between carbon and oxygen, the one which actually occurs at a given temperature is the one which has the more negative $\Delta G°$. From the Figure

6.14 it was noted that at lower temperatures (<700°C) the equilibrium is on the exothermic carbon dioxide side and at higher temperatures the endothermic formation of carbon monoxide is the dominant product. Figure 6.14 further showed that the formation of CO_2 by oxidation of carbon is constant and independent of temperature, while the formation of CO is a decreasing line.

In the region of 700°C, the two reactions (91 and 92) have approximately equal $\Delta G°$ values (the two lines intersect). This means that the products of combustion will be a mixture of CO and CO_2.

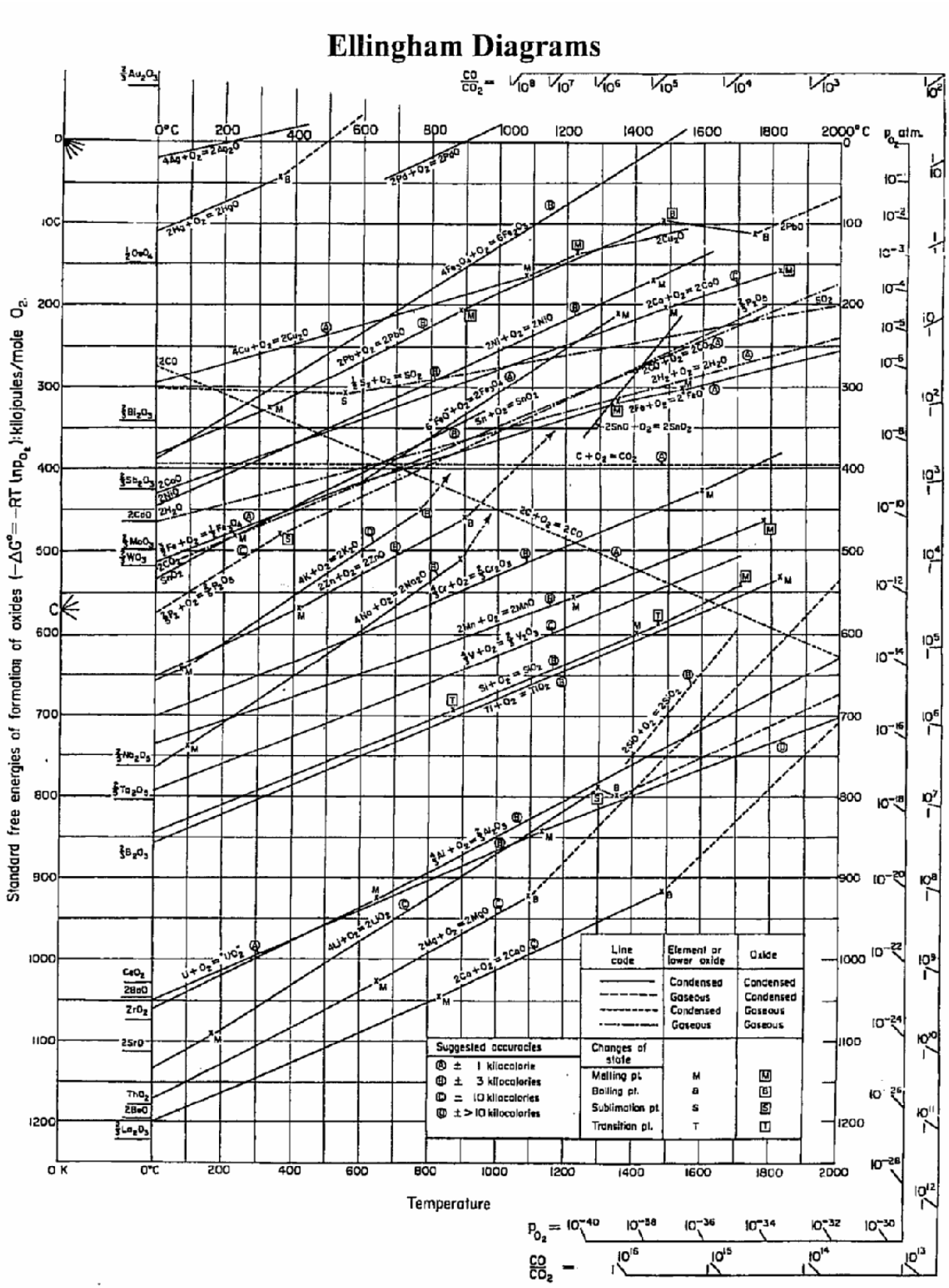

Figure 6.14 Scan of Ellingham diagram (Gaskell, 1993)

6.1.4 Isothermal studies

The isothermal experiments for the reaction between activated carbon and pure gypsum were conducted at the following temperatures: 800 °C, 850 °C, 900 °C, 925 °C, 950 °C, 975 °C and 1 000 °C . Figure 6.15 depicts the curves obtained for degree of conversion plotted against time at different temperatures. Different kinetic equations (as described in section 2.4.3) were used to distinguish the reaction mechanisms under isothermal conditions. Kinetic equations exist between the reacted fraction (α) and the time (t) for heterogenous reaction under isothermal conditions. For this study, the kinetic equations applicable when the rate-limiting process is diffusion and when it is a reaction at the phase boundary between the reactant and the reaction product were used, for example:

$$1-(1-\alpha)^{1/3} = kt \quad (95)$$

$$1-(1-\alpha)^{1/2} = kt \quad (96)$$

$$\left[1-(1-\alpha^{1/3})\right]^2 = kt \quad (97)$$

When the data were fitted in the above kinetic equations, a non-linear shape of the Arrhenius curve was obtained. This confirmed that the thermal decomposition of gypsum in the presence of carbon is not a single-stage reaction but rather a complex process.

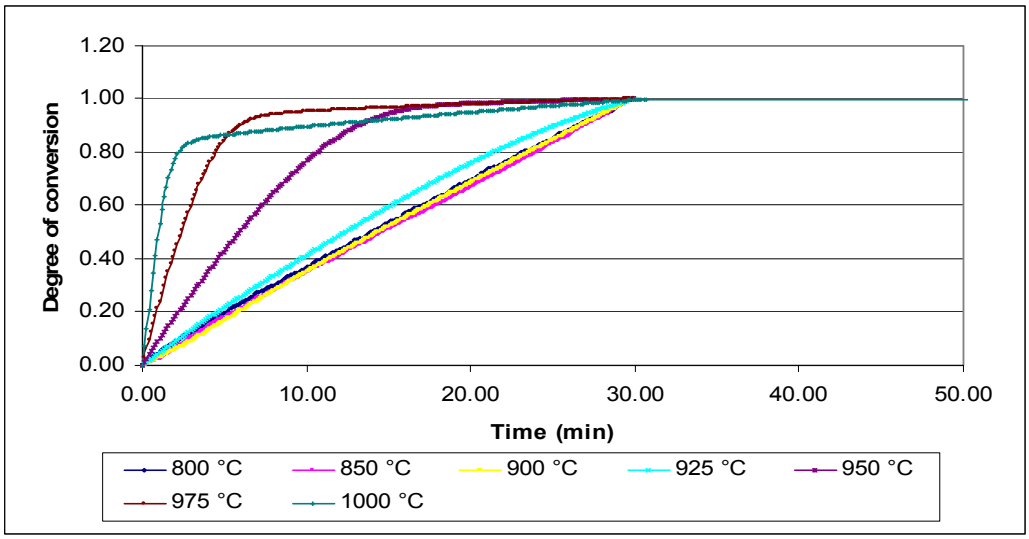

Figure 6.15 Plot of degree of conversion versus time for the reaction between activated carbon and pure gypsum under different isothermal conditions

Table 6.4 shows the mass losses obtained from thermogravimetric analysis of the reaction between activated carbon and pure gypsum at different temperatures. The results indicated that when the sample was heated at 800 °C, 21.1% mass was lost. However, increasing the temperature to 1 000 °C resulted in an increase in the mass loss to 64.8%. This result showed that the reaction between carbon and gypsum is temperature dependent and is favoured at high temperature.

Table 6.4 Thermogravimetric results for the reaction between activated carbon and pure gypsum under different isothermal conditions

Temperature ºC	T_{min} ºC	T_{max} ºC	Total mass loss (%)
800	25	800	21.1
850	25	850	23.4
900	25	900	42.6
925	25	925	59.1
950	25	950	63.5
975	25	975	63.8
1000	25	1000	64.8

6.2 SOLUBILITY OF CaS

Figures 6.16 and 6.17 show the results when the effects of stirring and temperature on the solubility of CaS were investigated. Initial sulphide concentrations for stirring and temperature studies were 270 mg/ℓ and 144 mg/ℓ, respectively. Sulphide dissolved in solution was measured as a function of time and temperature.

From Figure 6.16 it was noted that, the solubility of CaS increases from 270 mg/ℓ to 390 mg/ℓ with time 90 to 60 min. The increase in the solubility of CaS may be due to the oxygen available during stirring. Garcia- Calzada *et al.,* (2000) showed that oxygen accelerates CaS solubility due to the oxidation of HS^- to SO_3^{2-} and SO_4^{2-}

However, increasing the time from 60 min to 180 min did not show much change in the dissolved sulphide. The sulphide measured was approximately 390 mg/ℓ. The findings confirmed the low solubility of CaS.

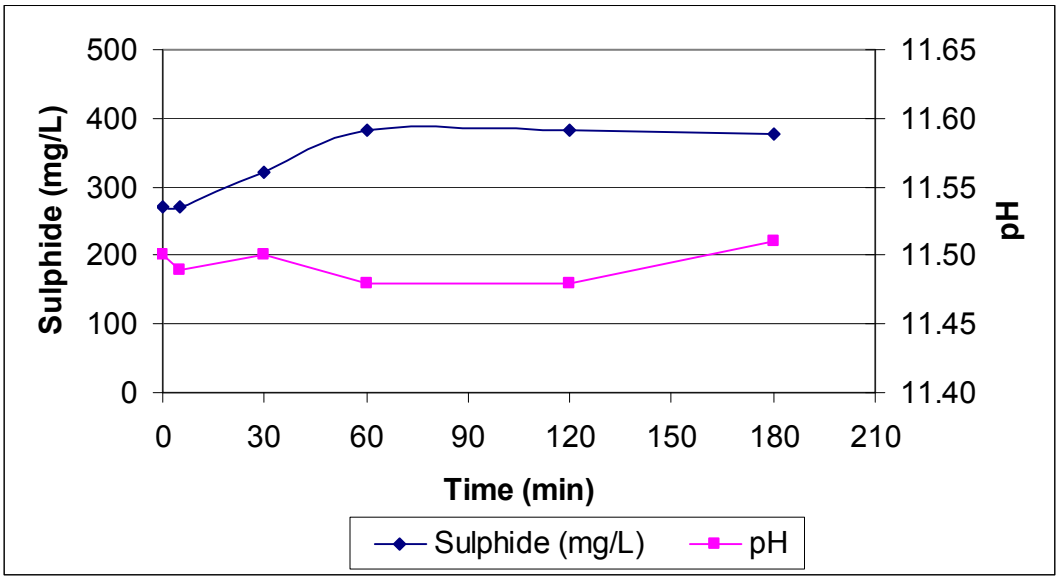

Figure 6.16 Effect of stirring on CaS solubility

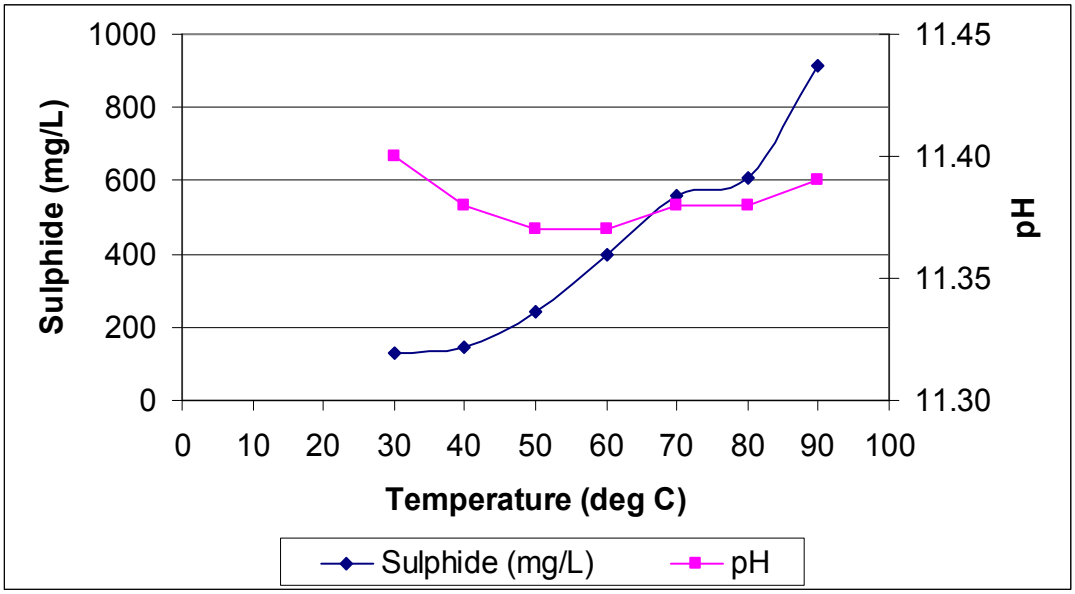

Figure 6.17 Effect of temperature on the CaS solubility

Figure 6.17 shows the effect of temperature on the solubility of CaS. The results show that increasing the temperature of CaS slurry resulted in an increase in the solubility of CaS. The graph further showed that at low temperature (30 °C-40 °C), the sulphide quickly dissolves to saturation. When the temperature was increased from 40 °C to 90 °C, the solubility of CaS increased from 144 mg/ℓ to 915 mg/ℓ.

The pH graphs from the above two figures (Figures 6.16 and 6.17) showed that when CaS was slurried in water, the pH value of the slurry was above 11. The higher pH value is due to the formation of $(CaOH)^{+}_{(aq)}$ (reaction 98) which is very basic. And for as long as there is no CO_2 gas available to strip the sulphide from CaS slurry, the pH will stay high. Garcia- Calzada (2000) further showed that at pH > 10, the sulphide is present as $HS^{-}_{(aq)}$. At pH < 10, sulphide is present as H_2S gas.

$$CaS\ (s) + H_2O\ (aq) \rightarrow (CaOH)^{+}\ (aq) + HS^{-}(aq) \qquad (98)$$

6.3 REACTION MECHANISM FOR SULPHIDE STRIPPING

The following study was conducted with the aim to investigate the reaction mechanism for the sulphide stripping from CaS slurry with CO_2 gas.

6.3.1 Behaviour of sulphide, calcium, alkalinity and pH during the sulphide stripping process

Figure 6.18 shows the time dependent behaviour of sulphide, calcium, alkalinity, CO_2 fed and pH during the sulphide stripping process. The initial CaS concentration was 1 083 mmol/ℓ and the CO_2 flow-rate, 520 mℓ /min.

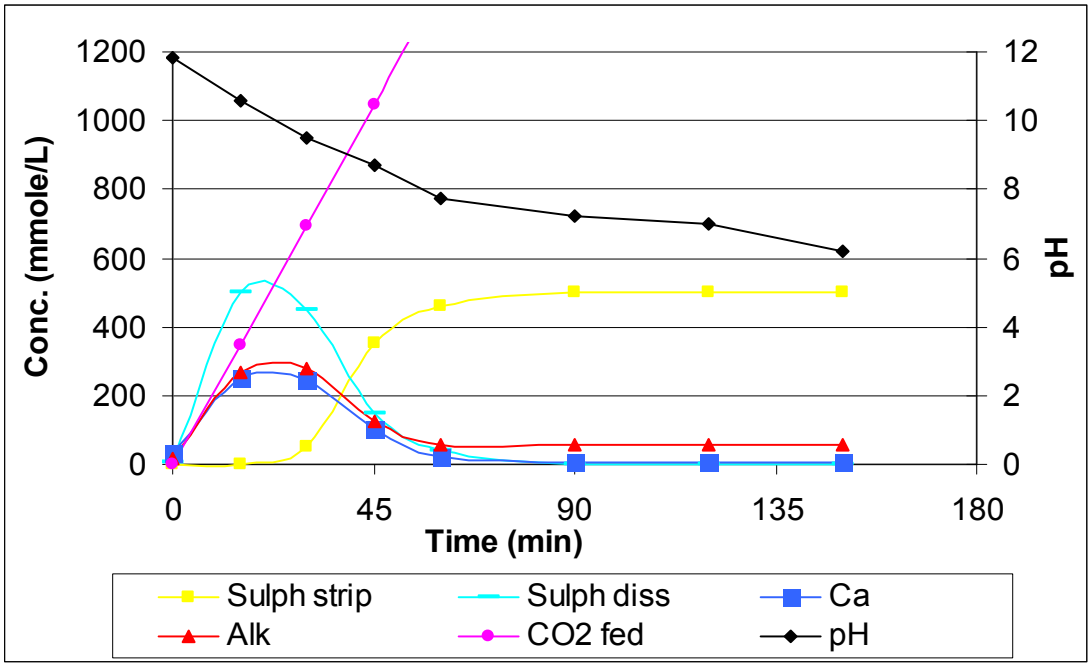

Figure 6.18 Behaviour of calcium, pH and sulphide during the sulphide stripping process with CO_2

The influence of the following parameters on the stripping process was noted from their representative graphs in Figure 6.18:

- ***Sulphide dissolved and stripped***

The graphs showed that during the first 30 min of the experiment, as CO_2 was passed through the CaS slurry, CaS dissolves to form $Ca(HS)_2$ (proposed intermediate, reaction 99). As more CO_2 (after 30 min) was added, the sulphide in the form of $Ca(HS)_2$ is decomposed and stripped off as H_2S gas (reaction 100). The graphs further showed that from the 1083 mmol/ℓ of sulphide as CaS that was initially slurried, only 510 mmol/ℓ sulphide dissolved

and stripped with CO_2. An investigation was carried out to explain why only 510 mmol/ℓ of sulphide dissolved and stripped. The results will be discussed in the following section.

$$2CaS\ (s) + CO_2\ (g) + H_2O\ (aq) \rightarrow CaCO_3\ (s) + Ca(HS)_2\ (aq) \quad (99)$$

$$Ca(HS)_2\ (aq) + CO_2\ (g) + H_2O\ (aq) \rightarrow CaCO_3\ (s) + 2H_2S\ (g) \quad (100)$$

- ***Calcium and Alkalinity***

The calcium graph showed that 250 mmol/ℓ of calcium was in solution and the alkalinity (an indication of the CO_3^{2-} concentration) was 270 mmol/ℓ. The concentrations of the two components (calcium and carbonate, reaction 101) were almost half the value of sulphide (as $Ca(HS)_2$) in solution (510 mmol/ℓ). From reaction 99, $Ca(HS)_2$ is equivalent to 2 mol sulphide as CaS but 1 mol $CaCO_3$ (reaction 99). The above finding indicates the formation of $Ca(HS)_2$. Furthermore, the low Ca concentration shows that $CaCO_3$ precipitates out due to its low solubility at pH values of 7.5 and higher.

$$Ca^{2+} + CO_3^{2-} \rightarrow CaCO_3\ (s) \quad (101)$$

- ***pH***

The pH graph indicates that when CO_2 is passed through a CaS slurry, the pH drops from 11.8 to 6.2. It was further concluded that above pH 10, sulphide is in solution as $Ca(HS)_2$ and below pH 10 it is present as H_2S gas (reaction 99 and 100, respectively) .

6.3.2 Analysis of the dissolved and suspended sulphide

Figure 6.19 depicts the experiment conducted with the aim to explain why only half of the initial sulphide slurried was measured (as dissolved and stripped) during the stripping process in the previous experiment (Figure. 6.18). The investigation was carried out using CaS slurry with an initial concentration of 1 200 mmol/ℓ and CO_2 at a flow rate of 520 mℓ/min. During the experiments, samples were taken and analysed. The sulphide analysis was done on the clear solution (filtrate) and on the mixed solution (filtrate and solids).

The results of analysing the two solutions showed that when sulphide was measured in the clear solution, only 650 mmol/ℓ sulphide concentration was present as dissolved sulphide. However, when sulphide was analysed from the mixture, 1 175 mmol/ℓ of sulphide was in suspension. The graph further showed that from the initial CaS concentration of 1 200 mmoe/ℓ, 1 175 mmol/ℓ of sulphide was stripped off with CO_2 gas. The difference of 25 mmol/ℓ sulphide may have escaped during the experiment. The finding indicated that during the stripping of sulphide from CaS slurry with CO_2, sulphide exists in solution as $Ca(HS)_2$ (aq) and is also present as solid $Ca(HS)_2$ (s). This demonstrates the low solubility of $Ca((HS)_2$.

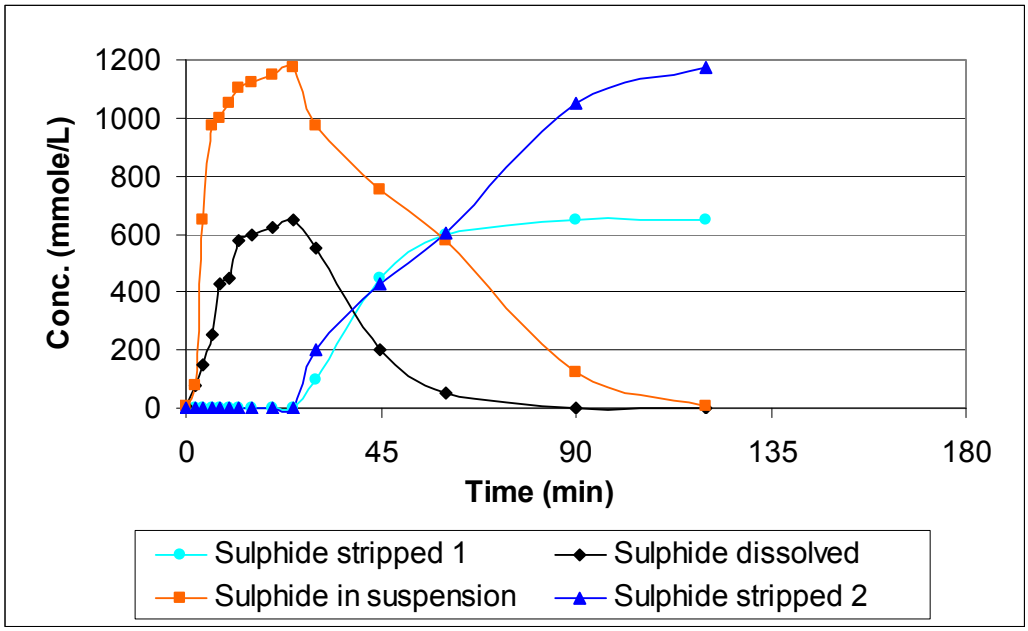

Figure 6.19 Analysis of the dissolved and suspended sulphide

6.4 SULPHIDE STRIPPING USING A PRESSURISED UNIT

Table 6.5 and Figures 6.20-6.23 illustrate the effect of various parameters (CO_2 flow-rate, temperature, pressure and hydrodynamics) on the rate of sulphide stripped, during the stripping of sulphide (as CaS) with CO_2. The experiments were carried out in a pressurised unit.

Table 6.5 Experimental conditions for the data reported in Figures 6.20-6.23

Parameters	Pressure (kPa)	Temp (°C)	Flow (ℓ/min)	Stirring Rate (r/min)
CO_2 flow	100	25	**2.22 (40%)**	1 000
	100	25	**3.34 (60%)**	1 000
Pressure	**100**	25	3.34	1 000
	200	25	3.34	1 000
Temperature	100	**25**	3.34	1 000
	100	**60**	3.34	1 000
Mixing intensity (r/min)	100	25	2.22	**500**
	100	25	2.22	**1 000**

The effect of the various parameters is discussed below.

Flow rate. The rate of sulphide stripped increased with increasing CO_2 flow-rates (Figure 6.20). The results showed that at high flow-rate (3.34 ℓ/min), more CO_2 gas entered the reactor to react with the CaS and as a result more sulphide (295 mmol) was being stripped. At low flow-rate (2.24 ℓ/min), it can be assumed that there was a sub-stoichiometric concentration of CO_2, and hence the amount of sulphide stripped was less (235 mmol).

Temperature. The rate of sulphide stripped increased with increased temperature (Figure 6.21). At 60 °C, 449 mmol/ℓ sulphide was stripped and at 25 °C only 297 mmol/ℓ. The results indicated that at higher temperature, more CaS was converted to $Ca(SH)_2$ and hence more sulphide was stripped off with CO_2. At lower temperature less CaS was converted and less sulphide was stripped.

Stirring rate. The rate of sulphide stripping increased with increased stirring rate (Fig. 6.22). When the stirring rate was 500 rpm, the amount of sulphide stripped was 245 mmol/ℓ. Stirring the CaS slurry at 1 000 rpm, the sulphide stripped increased to 565 mmol/ℓ. A function of the reactor design was such that when the stirring rate was increased it allowed for more of the gas in the headspace above the liquid to be sucked into a stirring vortex formed around the mixer shaft and contacted with the liquid. Through an increased stirring rate, there is improved mixing/contacting between the stripping gas (CO_2) and the dissolved sulphide as $Ca(HS)_2$, resulting in a faster rate of reaction.

Pressure. The rate of sulphide stripping increased with a decrease in pressure (Figure 6.23). When the pressure of CO_2 was 100 kPa, the sulphide stripped was 297 mmol/ℓ. However, when the pressure was increased to 200 kPa, the sulphide stripped decreased to 167 mmol/ℓ. This finding was attributed to the solubilities of CO_2 and H_2S that increased with increased pressure thereby decreasing the amount of CO_2 available for stripping the sulphide.

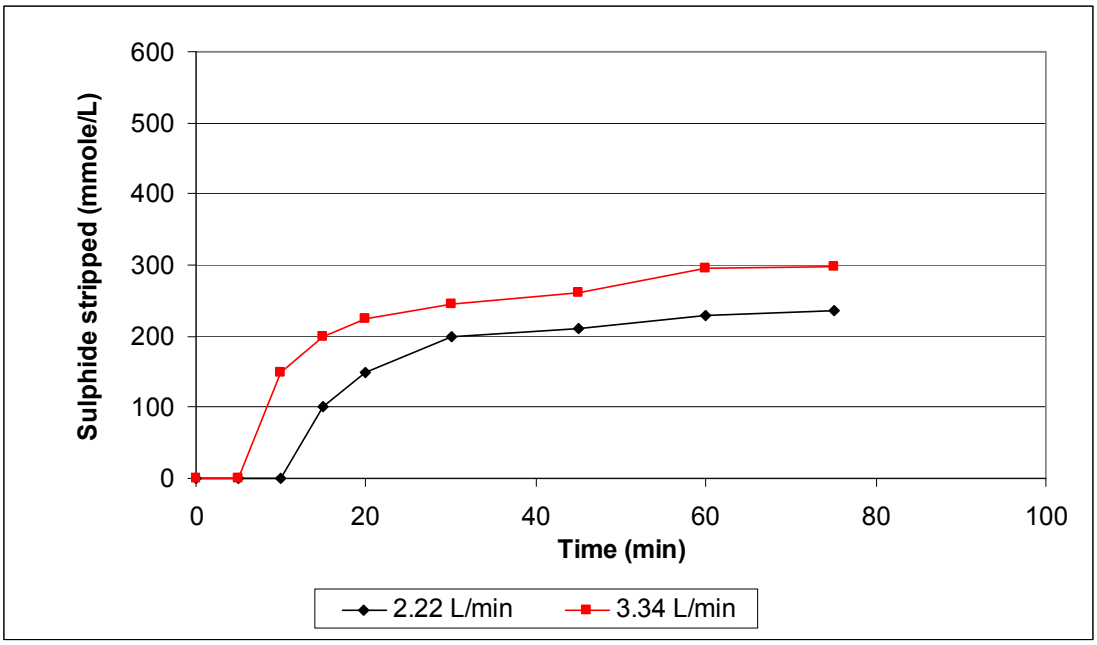

Figure 6.20 Effect of CO_2 flow rate on the sulphide stripping

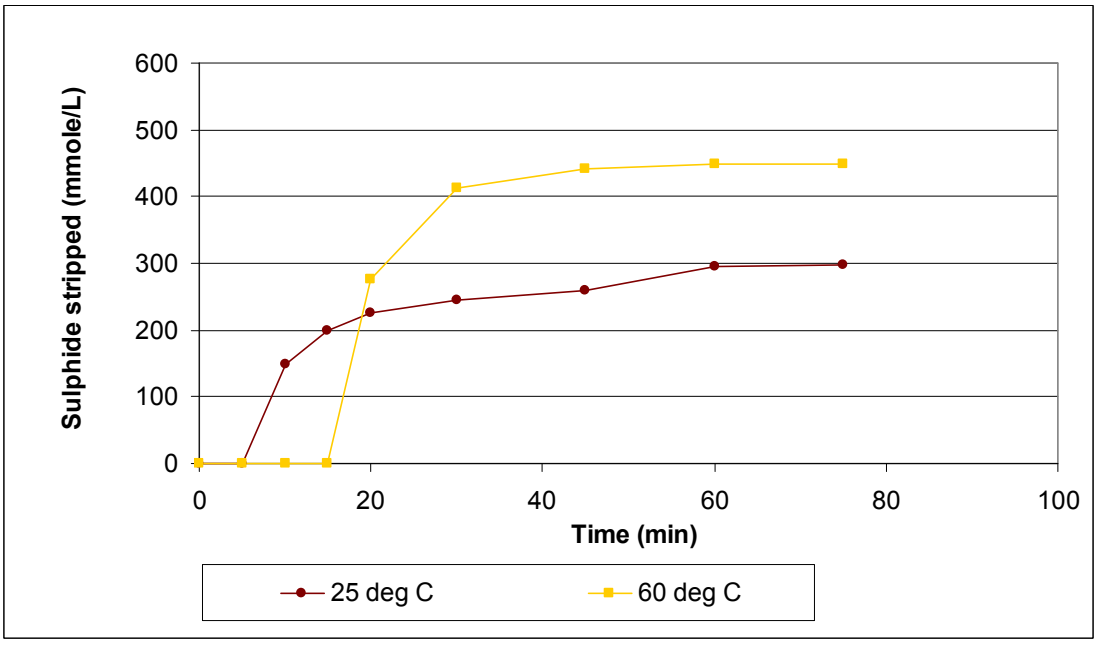

Figure 6.21 Effect of temperature on the sulphide stripping

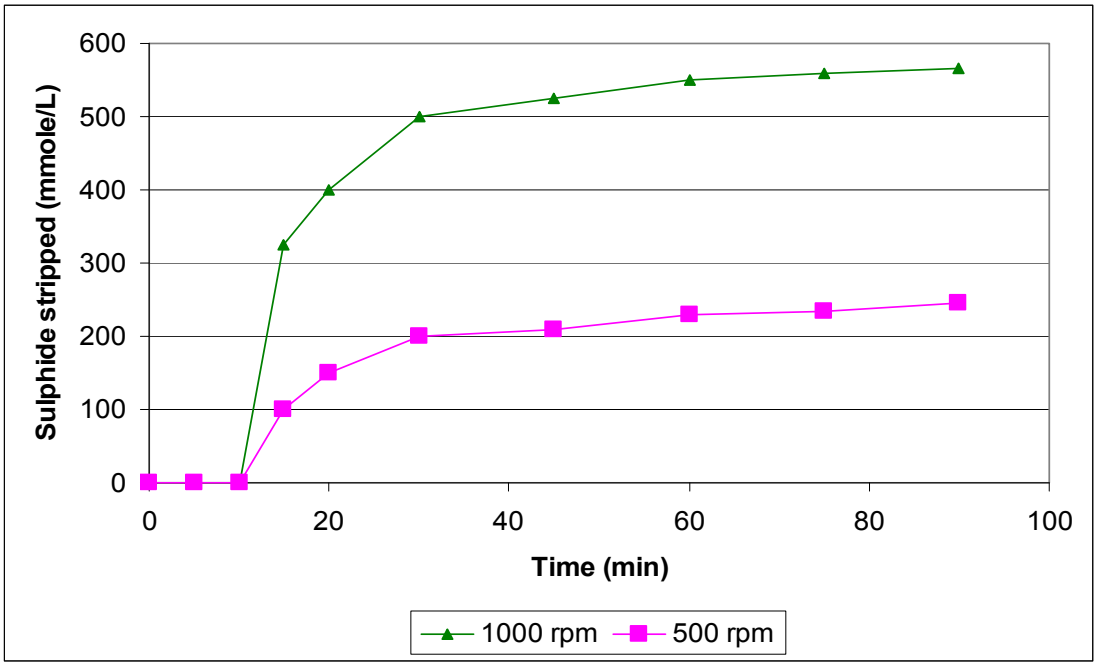

Figure 6.22 Effect of hydrodynamics on the sulphide stripping

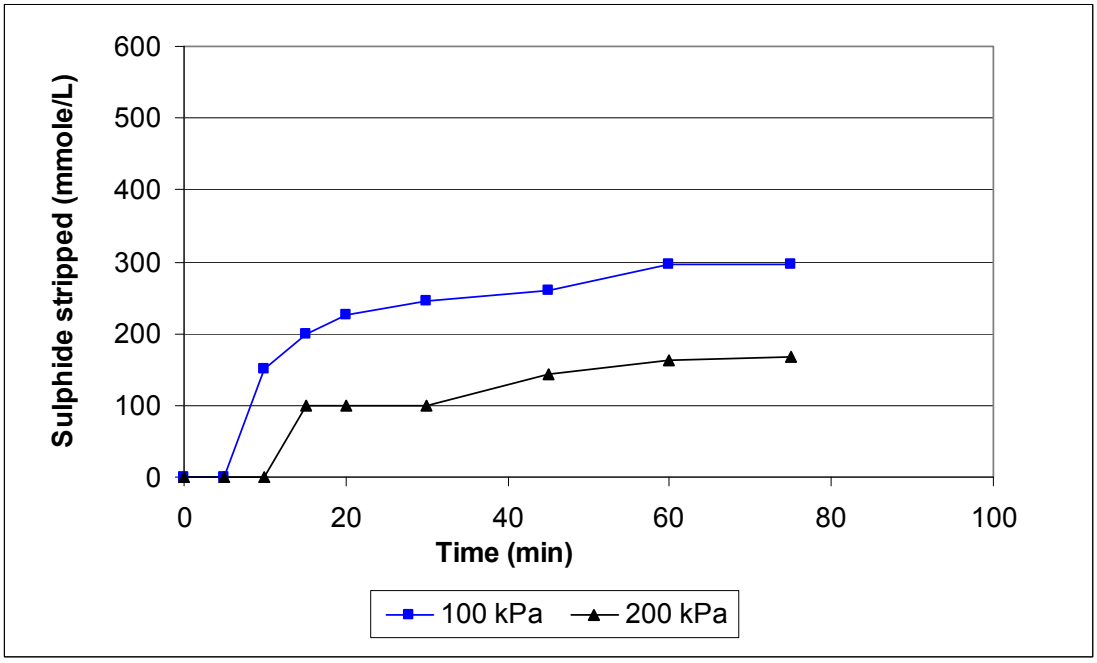

Figure 6.23 Effect of pressure on the sulphide stripping

6.5 H_2S GAS ABSORPTION AND SULPHUR FORMATION

This study was done to obtain an effective method for H_2S gas absorption and sulphur recovery. The two methods tested were the iron (III) process and the PIPco process.

6.5.1 Iron (III) process

This method involves the absorption of H_2S gas into an iron (III) solution (reaction 102). Figure 6.24 shows the time dependent behaviour of sulphide stripped load, pH, sulphur formed load and the CO_2 dosed load during the iron (III)-process.

$$H_2S\ (g) + 2Fe^{3+}\ (aq) \rightarrow S\ (s) + 2Fe^{2+}\ (aq) + 2H^{+}\ (aq) \qquad (102)$$

Similar conclusions were drawn from the behaviour of pH and sulphide as indicated in Section 6.3. For example, the pH decreases when sulphide is stripped with CO_2 and CaS dissolves as $Ca(HS)_2$ (aq). The sulphur curve showed that at 20 min reaction time, 113 mmol/ℓ of sulphide was stripped with CO_2 gas but only 8 mmol/ℓ of sulphur was formed in the iron (III) solution. This difference between the sulphide and sulphur formed can be explained in terms of a proposed, intermediate FeS complex that forms in the presence of iron (III) and H_2S gas. During the initial period (45-90 min) the sulphide stripped increased from 129 mmol/ℓ to 133 mmol/ℓ but the sulphur amount only increased from 36 mmol/ℓ to 51 mmol/ℓ. From the XRF results, it was found that 51% of the stripped H_2S was converted to elemental sulphur. The sulphur obtained from this study was brown. The investigation was stopped because more steps are required to purify the product.

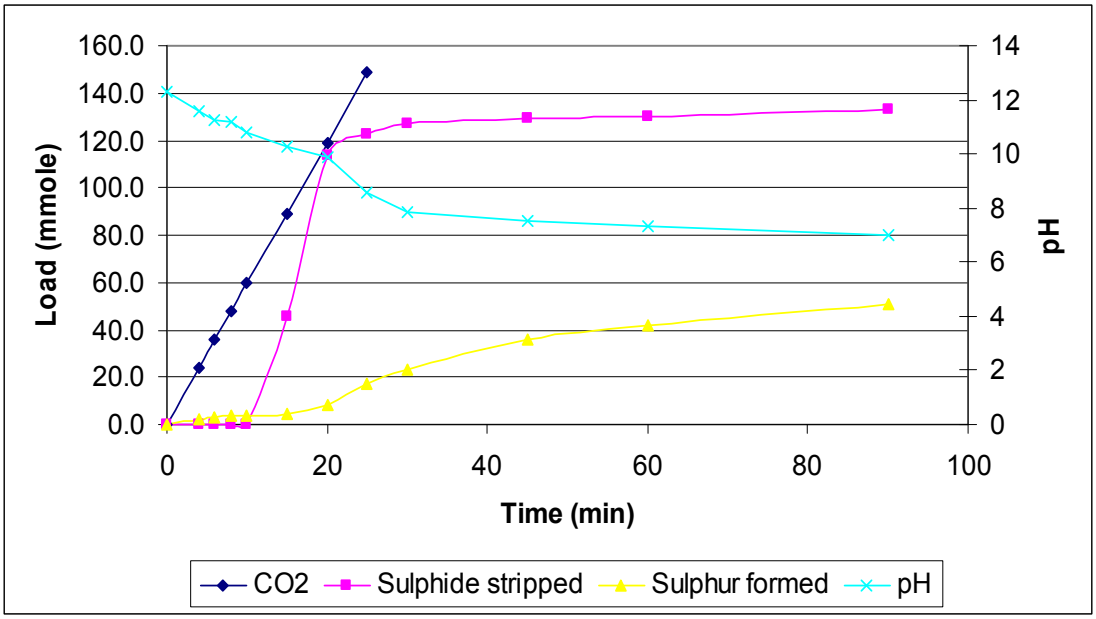

Figure 6.24 Behaviour of sulphide stripped, pH, sulphur formed and the CO_2 dosed during the iron (III)-process.

6.5.2 PIPco Process

In the PIPco process, H_2S gas is converted to sulphur, by reacting it with SO_2 gas in solution (reaction 103).

$$2H_2S\ (g) + SO_2\ (g) \rightarrow 3S\ (s) + 2H_2O\ (aq) \qquad (103)$$

The experiments reported in this section were carried out to establish optimum pH values and solubilities.

6.5.2.1 Effect of pH and concentration of potassium citrate on the absorption of SO_2 gas

Figures 6.25-6.27 depict the results obtained when the influence of pH, on different potassium citrate solutions for SO_2 gas absorption, was studied. The concentration of the citrate solutions was varied from 0.5 M to 1 M to 2 M, temperature was 25 °C and the gas flow-rate was 300 mℓ /min.

The results showed that for the different concentrations of potassium citrate (2 M, 1 M and 0.5 M) the pH decreases due to the absorption of acidic SO_2 gas which is acidic. However, it was further noted that in the beginning of the process, when the pH was still above 3, the rate of absorption was high and as the pH dropped, the absorption rate also decreased. This showed that the absorption of SO_2 if favoured by a pH higher than 3. At very low pH values the gas will remain in the gaseous form and no absorption will occur in the citrate solution.

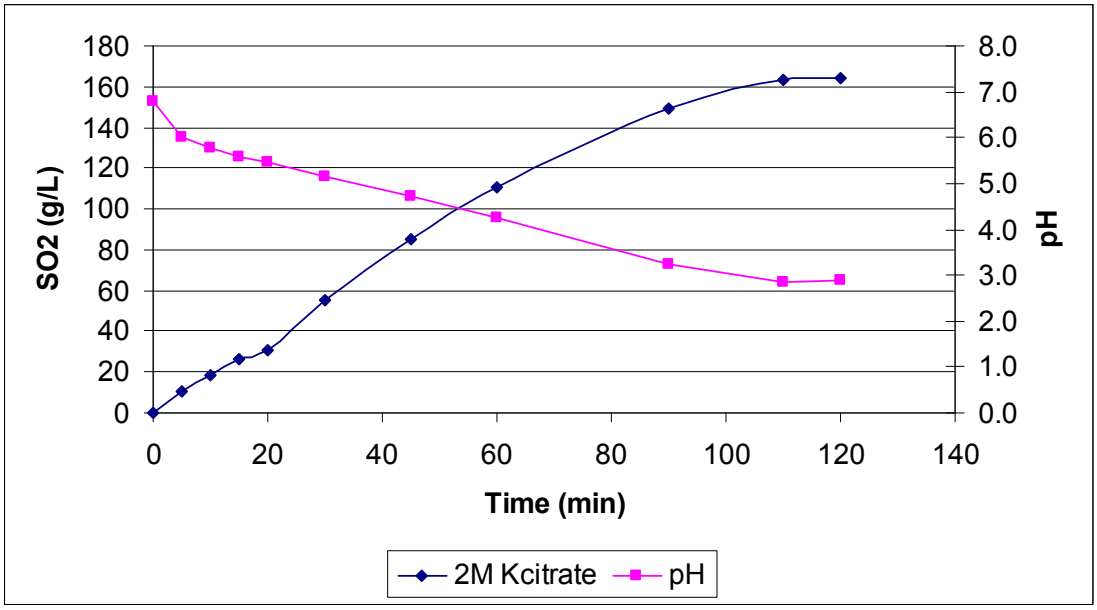

Figure 6.25 Effect of pH and 2 M of potassium citrate on the absorption of SO_2 gas

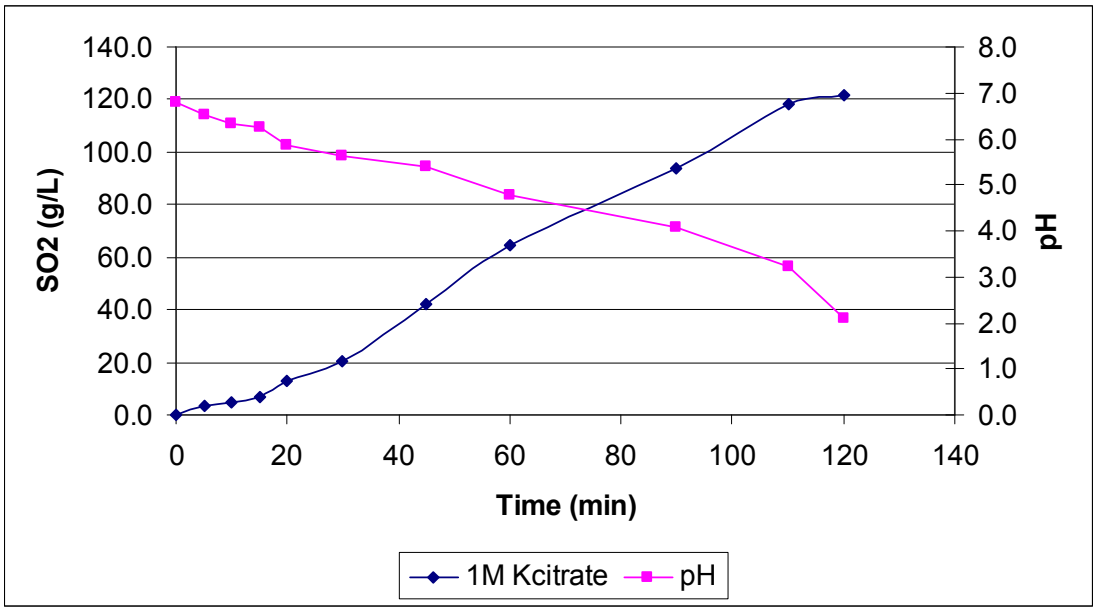

Figure 6.26 Effect of pH and 1M of potassium citrate on the absorption of SO_2 gas

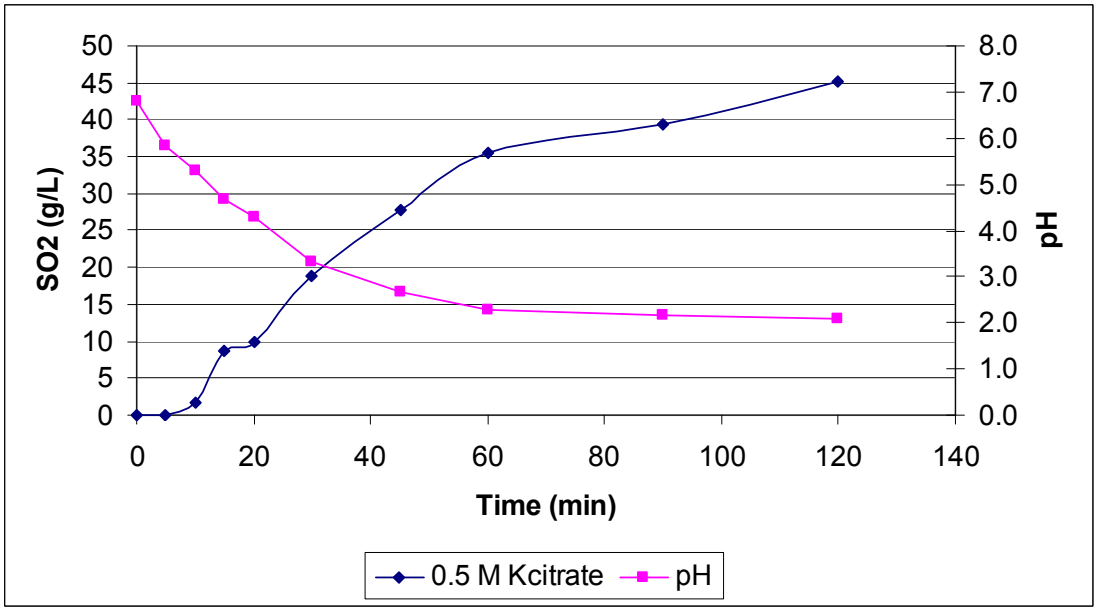

Figure 6.27 Effect of pH and 0.5M of potassium citrate on the absorption of SO_2 gas

The results depicted in Figures 6.25-6.27 further showed that with 2.0 M potassium citrate solution, the absorption of SO_2 gas was 164 g/ℓ after 120 min. However, when the potassium citrate concentration was low at 1.0 M and 0.5 M, the absorption decreased to 121 g/ℓ and 45 g/ℓ, respectively.

These findings showed that the absorption capacity is higher for solutions of higher citrate buffer concentration because of correspondingly larger buffer capacities. Therefore as more buffer capacity is available, more hydrogen ions formed in reaction 105 can bind to the citrate ions and be 'removed' by the buffer. The finding corresponded well with published capacity of 120-170 g/ℓ of SO_2 for 2 M potassium citrate solution (Gryka, 1992).

SO_2 (g) + H_2O (aq) → HSO_3^- (aq) + H^+(aq) (104)

Cit^{3-} (aq) + H^+ (aq) → $HCit^{2-}$ (aq) (105)

$HCit^{2-}$ (aq) + H^+ (aq) → H_2Cit^- (106)

6.5.2.2 Effect of temperature on the absorption of SO_2 in citrate buffer

Figure 6.28 shows the influence of temperature on the absorption of SO_2 in a 2 M potassium citrate solution at pH 6.8.

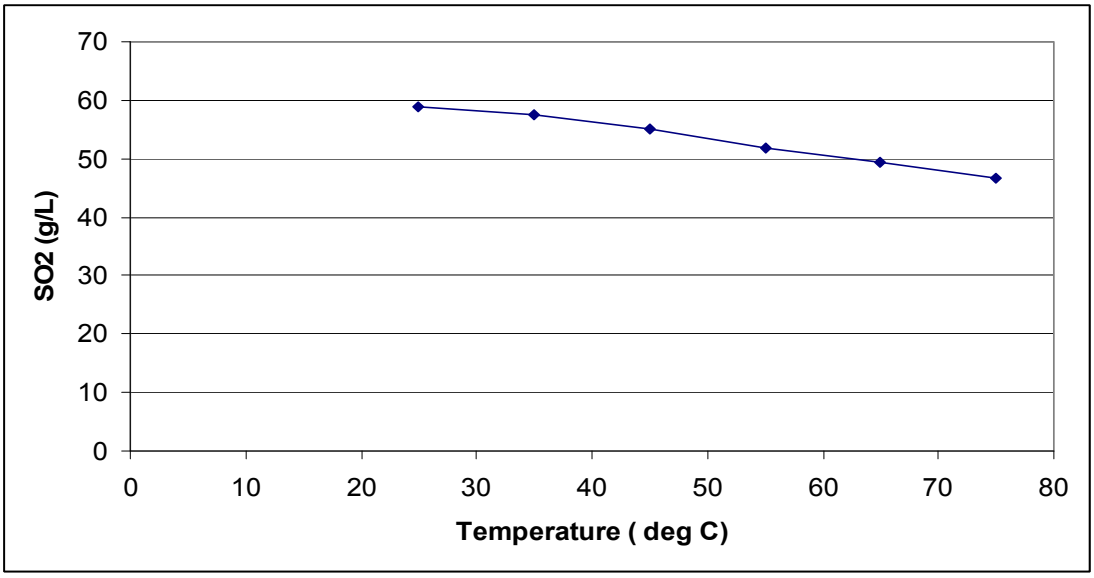

Figure 6.28 Effect of temperature on SO_2 absorption into a potassium citrate solution

The results showed that when the temperature of the potassium citrate solution was 25 °C, the SO_2 absorbed was 59 g/ℓ. When the temperature was increased from 35 °C to 75 °C, the SO_2 absorption decreased from 58 g/ℓ to

47 g/ℓ. These results showed that the solubility of SO_2 decreases with increasing temperatures. Gryka (1992) showed that the absorption of SO_2 into a potassium citrate solution should take place at a temperature as low as possible.

6.5.2.3 Solubility of H_2S in Potassium Citrate buffer solution

Figure 6.29 shows the relationship between H_2S loaded and H_2S absorbed in a 2 M potassium citrate buffer solution at ambient temperature and atmospheric pressure. Even though 800mmol/l of H_2S was fed to the system only 24 mmole/ℓ (752 mg sulphide/ℓ) was absorbed in the first citric acid solution and 17 mmole/ℓ (544 mg sulphide/ℓ) in the second. Therefore, at atmospheric pressure and ambient temperature, the solubility of H_2S in potassium citrate buffer solution is very low, only between 2% to 3%.

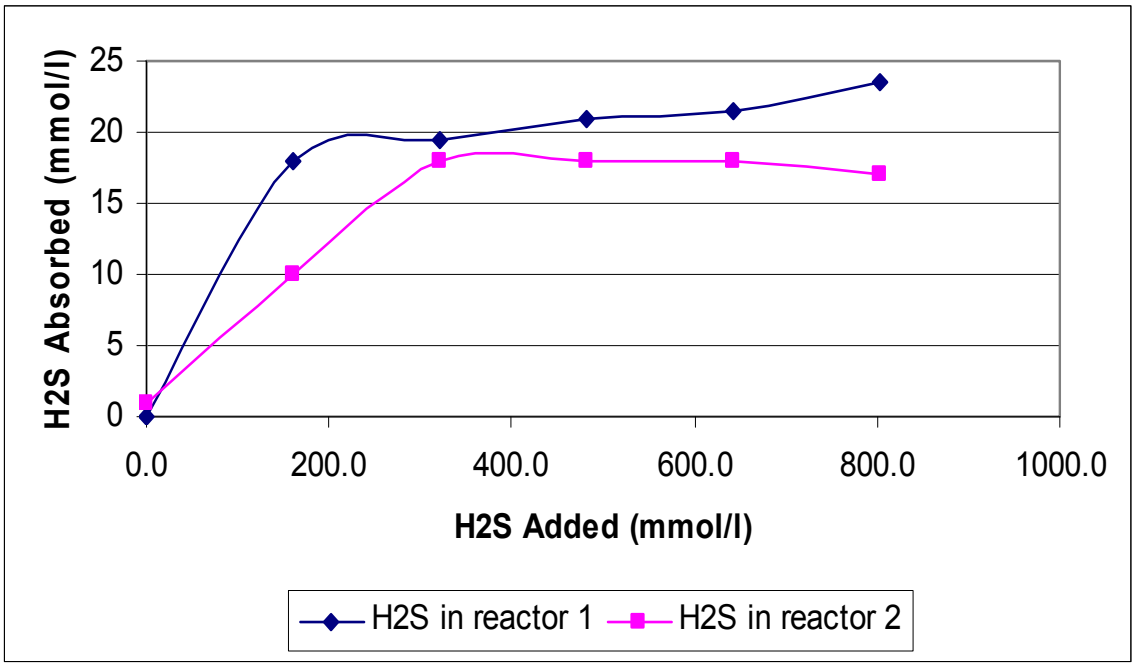

Figure 6.29 Solubility of H_2S gas in potassium citrate buffer solution

6.5.2.4 Sulphur production via the PIPco process

The purpose of this section is to determine the effect of CO_2 flow rate on the formation of intermediate compounds during sulphur production via the PIPco process.

Figures 6.30-6.33 and Tables 6.6 and 6.7 show the results, as well as the experimental conditions, when sulphide was stripped with CO_2 from a CaS slurry, followed by absorption of the stripped H_2S gas in a SO_2-rich potassium citrate solution for sulphur formation. The effect of CO_2 flow rate was investigated by experiments at 520 mℓ/min and at 1112 mℓ/min.

Figure 6.30 shows the relationship between the concentrations of the various species versus time when CO_2 was passed through at a flow-rate of 520 mℓ/min. The initial CaS concentration in the slurry was 2 167 mmol/ℓ and the pH was 12.2. The sulphide level in solution was 3.0 mmol/ℓ before the addition of CO_2.

During CO_2 addition the pH dropped from 12.2 to 8.2. The sulphide concentration in the slurry reactor dissolved until it reached a maximum concentration of 1 375 mmol/ℓ due to the formation of $Ca(HS)_2$. With further CO_2 addition, the pH dropped further to 6.9 and sulphide was stripped completely. The stripped H_2S reacted with the SO_3^2 in citrate reactors. The SO_3^{2-}concentration in Reactor 1 dropped sharply, while in Reactor 2 it dropped slowly. The rapid drop in Reactor 1 was ascribed to the formation of sulphur and possibly to some of the SO_2 being stripped with CO_2. The slow drop in the SO_3^{2-}-concentration in Reactor 2 was ascribed to SO_2-stripping with CO_2.

From Figure 6.31, which shows the relationship between load (accumulated amount) removed or formed of the various parameters as a function of time, it was noted that:

- 2 167 mmol CaS was initially slurried.
- 1 375 mmol of the $Ca(HS)_2$ formed was in solution and the balance was present as a solid as the solubility of $Ca(HS)_2$ was exceeded (Section 6.3.2).

- 2 180 mmol SO_3^{2-} was removed, which is more than the concentration of CaS that was slurried. This showed that a portion of the SO_2 was stripped with CO_2. This observation explains why the PIPco process needs to be operated under excess H_2S-conditions.

The experiment described above for 520 mℓ/min CO_2 was repeated for a CO_2 flow rate of 1 112 mℓ/min (Figures 6.32 and 6.33 and Table 6.7). Similar conclusions were drawn except for the behaviour of SO_3^{2-} in the SO_2/citrate reactor. The following similar observations were made:

- 2 167 mmol CaS was initially slurried.
- 1 300 mmol dissolved in solution as $Ca(HS)_2$, and the balance was in solid form as $Ca(HS)_2$.
- 2 310 mmol SO_3^{2-} was removed which is more than expected from the amount of CaS that was slurried. This shows that a portion of the SO_2 was stripped with CO_2.

The following differences were observed between the two CO_2 flow-rates studies: The increase in SO_3^{2-}-concentration during the initial period (Figure 6.32) was ascribed to the formation of an intermediate compound when H_2S was reacted with the SO_2/citrate solution. This compound is oxidised to sulphate from a much lower valence (valence of S species) when reacted with iodine, compared to SO_3^{2-}, which has a valence of +4. The intermediate could be $S_3O_4^{2-}$, with a valence of +2. Reaction 107 shows the reaction of $S_3O_4^{2-}$ with iodine. This was determined by way of elimination of the reactions with iodine of the various sulphur species.

- $S_2O_3^{2-}$ is oxidised to $S_4O_6^{2-}$ (reaction 79) and the latter will not be further oxidised with iodine
- SO_3^{2-} is oxidised to SO_4^{2-} (reaction 78)
- Thus, $S_3O_4^{2-}$ is the only remaining sulphur species and can only be oxidized to SO_4^{2-}. I

$$S_3O_4^{2-}(aq) + 6I_2(aq) + 8H_2O(aq) \rightarrow 3SO_4^{2-}(aq) + 12I_2(aq) + 16H^+(aq) \quad (107)$$

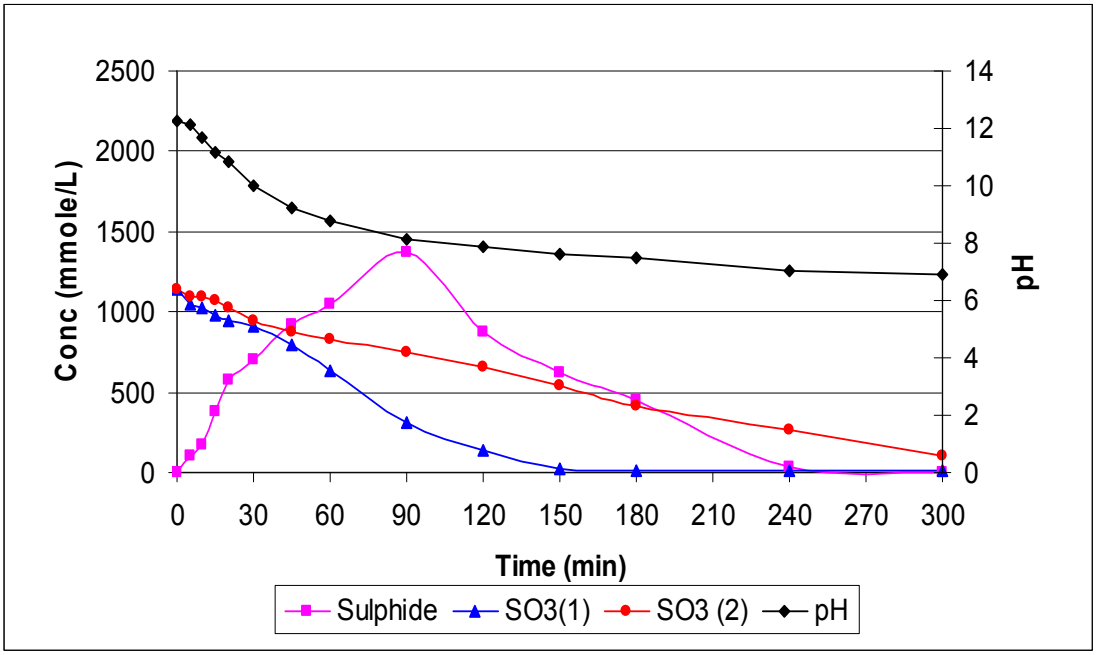

Figure 6.30 Sulphide stripping with CO_2 gas at a flow rate of 520 mℓ/min (concentrations versus time).

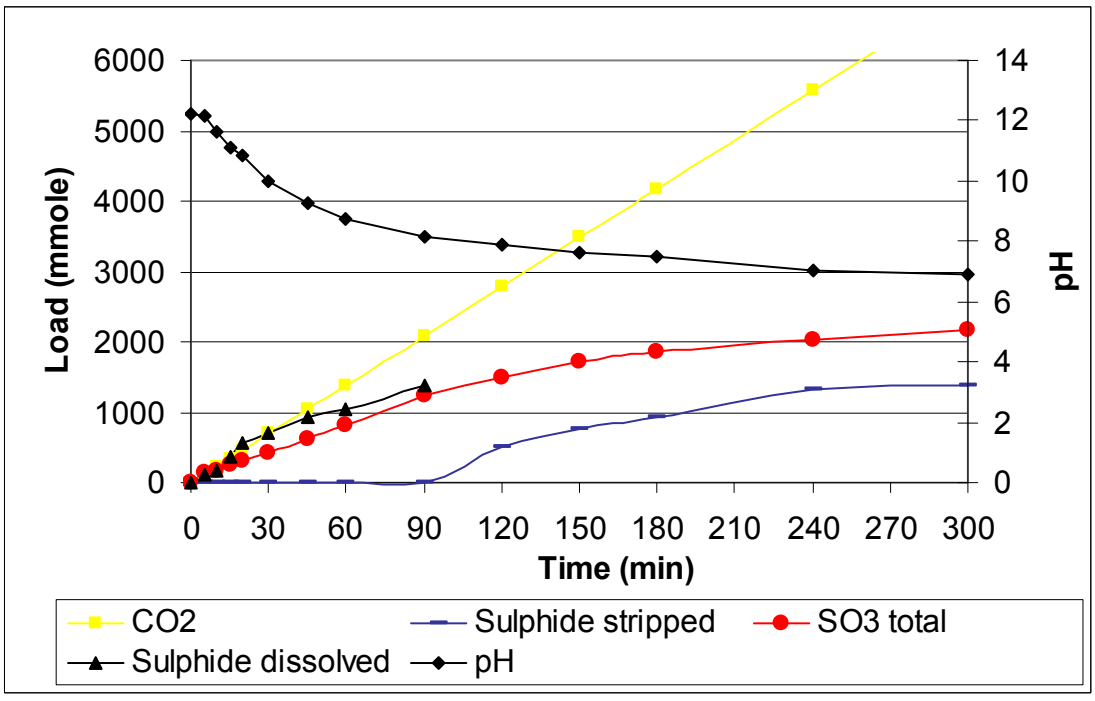

Figure 6.31 Sulphide stripping with CO_2 gas at a flow rate of 520 mℓ/min (load versus time).

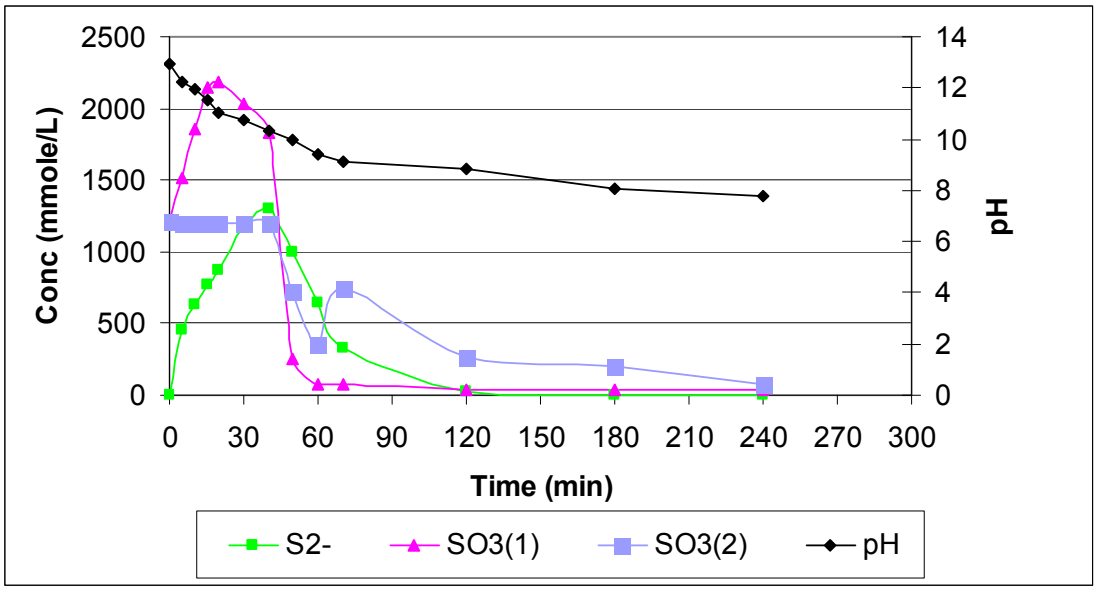

Figure 6.32 Sulphide stripping with CO_2 gas at a flow rate of 1112 mℓ/min (concentrations versus time).

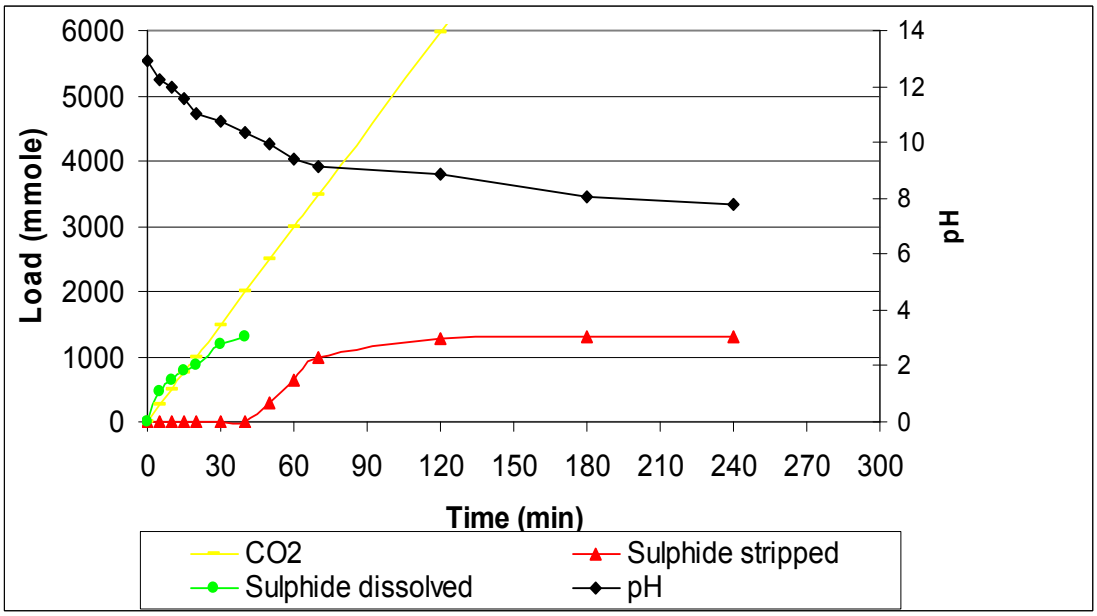

Figure 6.33 Sulphide stripping with CO_2 gas at a flow rate of 1112 mℓ/min (load versus time).

Table 6.6 Sulphide stripping with CO_2 gas at a flow rate of 520 mℓ/min

Parameter	CaS reactor		SO_2/Citrate 1		SO_2/Citrate 2	
Time (min)	0	300	0	300	0	300
Citric acid (g/ℓ)			768		768	
KOH (g/ℓ)			673		673	
CO_2 (mL/min)	520					
CaS (mmole/ℓ)	2167					
Sulphide (mmole/ℓ)	2167	64				
SO_3^{2-} (mmole/ℓ)			1145	10	1145	100
pH	12.2	6.9				

Table 6.7 Sulphide stripping with CO_2 gas at a flow rate of 1112 mℓ/min

Parameter	CaS reactor		SO_2/Citrate 1		SO_2/Citrrate 2	
Time (min)	0	240	0	240	0	240
Citric acid (g/ℓ)			768		768	
KOH (g/ℓ)			673		673	
CO_2 (mℓ/min)	1112					
CaS (mmole/ℓ)	2167					
Sulphide (mmole/ℓ)	2167	16				
SO_3^{2-} (mmole/ℓ)			1215	40	1215	80
pH	12.9	7.8				

6.5.2.5 Purity of sulphur recovered

The LECO Combustion Techniques used to assay the purity of sulphur showed that sulphur with purity between 96 and 99% was recovered.

To identify the other elements formed during the recovery of sulphur, XRF analyses were conducted on the sulphur samples. The results are indicated in Table 6.8.

Table 6.8 Results of XRF analysis of recovered sulphur

Elements	Conc. Impurities
K	820 ppm
Fe	91 ppm
Ca	184 ppm
Mg	170 ppm
Si	20 ppm
Co	40 ppm
Cr	60 ppm
Ni	56 ppm

6.5.2.6 Economic feasibility

The recovery of sulphur and $CaCO_3$ from gypsum based on laboratory and pilot studies (pilot results not included in this study), seems to be economically feasible. From 1 ton of gypsum it was calculated that 0.18 ton of sulphur (Value = R180) and 0.58 t of $CaCO_3$ (Value = R145) can be recovered. The prices of sulphur and $CaCO_3$ were taken at R500/t and R250/t, respectively. This compares favourable with the cost of the main raw material, coal. At a coal to gypsum ratio of 0.3, and a coal cost of R400/t, the cost of the coal amounts to R120/t of gypsum. This is significantly less than the combined value of R296 of sulphur and $CaCO_3$. This value would be even higher if chemically pure $CaCO_3$ is recovered. The price of chemically pure $CaCO_3$ amounts to R3 000/t compared to the R250/t for waste or mined $CaCO_3$.

CHAPTER 7

CONCLUSIONS

7.1 THERMAL STUDIES

The thermal conversion of gypsum to CaS in a tube furnace and nitrogen atmosphere takes place between 900 °C-1 100 °C:

$$CaSO_4\ (s) + 2C\ (s) \rightarrow CaS\ (s) + 2CO_2\ (g) \qquad (108)$$

96% conversion gypsum to CaS was obtained when a reducing agent, carbon, was used. Controlling the amount of carbon added, relative to the amount of gypsum, higher reduction yields were achieved when the molar ratio of gypsum to carbon was 1:2 and 1:3. 380 µm particle size of gypsum yielded 80% reduction percentages due to the higher reactant surface areas for smaller particles.

The reaction time between gypsum and carbon was also found to be shorter. The optimum time found was 20 min. The impurities present in Anglo and Foskor gypsum seemed to lower the CaS yields as compared to pure gypsum. Regardless of the grade of Duff coal, which is low, 81% CaS yields were obtained when Duff coal was used as a reducing agent. Due to the high cost of activated carbon, Duff coal was recommended for use on a full-scale plant.

Depending on the presence of oxygen in the muffle furnace, the CaS obtained after heating the gypsum at 1 100 °C was contaminated by oxygen-containing compounds. The tube furnace which had been purged with nitrogen yielded none of these contaminants. The thermal decomposition of gypsum to CaS should therefore be carried out in an oxygen-deficient environment.

Thermogravimetric results showed that the loss of water of crystallisation from pure gypsum ($CaSO_4.2H_2O$) takes place in the temperature range 80 °C-180 °C. The small mass loss occurring between 650 °C-800 °C was attributed to the oxidation of carbon. The mass loss between 900 °C-1 050 °C confirmed the formation of CaS.

Kinetic analysis showed that complex reactions occurred between activated carbon/carbon monoxide and the three gypsum types (pure, Anglo and Foskor gypsum). This conclusion was made from the fact that the activation energies changed for different degrees of conversion. The increasing dependencies of activation energy on the degree of conversion were evidence for a complex reaction involving parallel reactions. The increase in activation energy at the initial stage (α < 0.2) of transformation shows parallel competing reactions.

Between the conversion degree of 0.2-0.75, a relative constant dependency of the activation energy on the degree of conversion showed that there is no change in the rate limiting step. This observation was claimed on different influence of diffusion of gaseous products. The presence of impurities in the Foskor and Anglo gypsums caused interferences owing to side reactions.

Solid–solid reactions are slow as compared to solid–gas reactions as evidenced by their higher activation energies. It was concluded that the reaction between activated carbon and gypsum could occur via the reaction product CO and CO_2 depending on the temperature. Below 700 °C, CO_2 is the dominant product while above 700 °C, CO is dominant.

The thermogravimetric data obtained during isothermal studies confirmed that the reaction between activated carbon and pure gypsum is complex because the data failed to give straight line graphs when fitted to different kinetic equations.

7.2 SOLUBILITY OF CaS

The solubility of CaS increased from 270 to 390 mg/ℓ with time 90 to 60 min, through stirring. Increasing the temperature from 30 °C-90 °C also increased the solubility of CaS from 130 mg/ℓ to 915 mg/ℓ. The high pH (pH>11) of a CaS slurry is due to the formation of $(CaOH)^{+}_{(aq)}$ which is very basic. At this high pH, sulphide is present as $HS^{-}_{(aq)}$.

7.3 REACTION MECHANISM FOR SULPHIDE STRIPPING

During the stripping of sulphide (as CaS) with CO_2 gas at 25 °C and atmospheric pressure, CaS reacts first to form an intermediate, $Ca(HS)_2$, before the sulphide is stripped off. Due to the low solubility of CaS, not all the sulphide dissolves as $Ca(HS)_{2(aq)}$ during the stripping process, a certain amount stays undissolved as $Ca(HS)_{2(s)}$. As more CO_2 is added, the sulphide which is in the form of $Ca(HS)_2$ is stripped off as H_2S gas:

$$2CaS\ (s) + CO_2\ (g) + H_2O\ (aq) \rightarrow CaCO_3\ (s) + Ca(HS)_2\ (aq,s) \qquad (109)$$

$$Ca(HS)_2\ (aq,s) + CO_2\ (g) + H_2O\ (aq) \rightarrow CaCO_3\ (s) + 2H_2S\ (g) \qquad (110)$$

The pH of the sulphide solution drops from pH 11 to 7 due to the formation of $CaCO_3$.

7.4 SULPHIDE STRIPPING USING A PRESSURISED UNIT

The rate of sulphide stripping can be increased by controlling the following parameters:

1) Flow rate

A high flow rate (3.34 ℓ/min) of CO_2 gas increased the rate of sulphide stripped to 295 mmol/ℓ compared to 235 mmol/ℓ for 2.24 ℓ/min.

2) Temperature

The increase in temperature from 25 °C to 60 °C resulted in an increase in the rate of sulphide stripping from 297 mmol/ℓ to 449 mmol/ℓ, respectively. This indicated that the solubility of CaS increases with temperature.

3) Stirring rate

The rate of sulphide stripped increased from 245 mmol/ℓ to 565 mmol/ℓ, when the stirring rate was 500 rpm and 1000 rpm, respectively. It was concluded that at a faster stirring rate, the contact between the CO_2 gas and sulphide species improves.

4) Pressure

The rate of the sulphide stripping increased with a decrease in pressure. At 100 kPa, the sulphide stripped was 297 mmol/ℓ and at 200 kPa, only 167 mmol/ℓ was stripped. The results showed that the solubility of CO_2 gas and H_2S gas increased at an increased pressure.

7.5 SULPHUR FORMATION

The two processes iron (III) and PIPco were investigated for sulphur recovery. The iron (III) method involves the absorption of H_2S gas into a iron (III) solution while in the PIPco, H_2S gas is absorbed into a potassium citrate solution rich in SO_2 gas for sulphur formation.

It was concluded that the iron (III) process yields poor quality sulphur. The sulphur recovered was brown in colour due to the presence of iron (III) and contained FeS. The purity of the sulphur was 51 %. No further work was done following this finding.

From the PIPco process, pure yellow sulphur with a purity between 96%-99% was recovered.

The following parameters are of importance in the PIPco process:

- ***pH***

The pH of the potassium citrate must be higher than 3 for better SO_2 absorption. At very low pH, the potassium citrate cannot absorb SO_2.

- ***Concentration of potassium citrate.***

The 2 M concentration of potassium citrate absorbs 164 g/ℓ of SO_2 gas within a period of 120 minutes while 1 M and 0.5 M absorbs 125 g/ℓ and 45 g/ℓ, respectively. It was concluded that the absorption capacity is higher for solutions of higher buffer concentration. The overall results showed that potassium citrate is a good absorbent for SO_2 gas.

- ***Temperature***

The results, as obtained from this study showed that optimum temperature for the absorption of SO_2 gas into the potassium citrate was 25 °C. At this temperature, 59 g/ℓ SO_2 was absorbed.

Increasing the temperature of the potassium citrate from 35 °C to 75 °C resulted in a decrease in the SO_2 gas absorption (from 58 g/ℓ to 47 g/ℓ, respectively).

It was further shown that the solubility of H_2S gas in the potassium citrate solution is very low, between 2%-3%. Therefore, during sulphur production, the H_2S gas will react with the SO_2 gas to form sulphur.

7.6 RECOMMENDATIONS

The aim of this project was to investigate, understand and optimize various stages of the sulphur recovery process on laboratory scale to the stage prior to full-scale implementation. The following recommendations are proposed for full-scale implementation:

- A rotating kiln must be used to heat gypsum to prevent lump formation.
- Gypsum must be dried to prevent lumps forming.
- Duff coal can be used as a reducing agent as well as a source of heat for the kiln because is readily available and cheap.
- To reduce the operation cost, propane can be used to pre-heat the kiln as opposed to electrical power.
- CaS from the kiln needs to be cooled before slurried to avoid boiling.
- To increase the rate of solubilisation of CaS during the stripping of sulphide, the CaS slurry should be stirred and heated at a temperature between 60 °C-90 °C
- The citrate solution must be buffered with KOH to control the pH at the optimum level for the following competing reactions:
    - Absorption of acid gasses, H_2S and SO_2, is favoured at higher pH values. At low pH values the gasses will remain in the gas form and no absorption will occur in the citric acid.
    - Sulphur formation which favour low pH occurs according to the reaction:

$$2HS^- + S_2O_3^{2-} + 4H^+ \rightarrow 4S + 3H_2O \qquad (111)$$

- Potassium citrate may be used for SO_2 absorption during sulphur production because it is a good absorbent for SO_2 gas

- The process temperature is controlled at 125 °C and the pressure at 3 bar to retain sulphur in liquid form and to prevent the water from evaporating.

7.7 PROPOSED PROCESS DESCRIPTION

The process description below is a proposed design to recover sulphur from the waste gypsum resulting from the treatment of acid mine drainage in the Key Plan water treatment plant to recover potable water for the Witbank Local Council.

1) Kiln

The main purpose of the kiln is to reduce the gypsum ($CaSO_4.2H_2O$) to CaS. The first step in the process is to dry the wet gypsum from about 25% moisture to about 10% and to blend it with Duff coal at a ratio of 26% (coal to dried gypsum). The coal acts both as a source of heat as well as a reductant in the kiln. The blended gypsum and coal mixture is stored in a “day” bin from where it is discharged into the kiln by a calibrated screw feeder. The kiln is pre-heated with propane to a temperature of 1100 °C. Combustion air is controlled to yield an off-gas CO concentration of 1.5 to 2%.

Gas analyses are carried out at regular intervals with the aid of a Testo analyzer (O_2 and CO). Hot gases from the kiln are cooled in a trombone radiation cooler to below 200 °C and filtered in the bagfilter. From the bagfilter approximately 1/3 of the gas is blown by the ID fan to the stack. Approximately 2/3 of the offgas is further cooled to about 35 °C and compressed to 5 Bar into a 2 m^3 pressure vessel.

CaS exits from the kiln at about 900 ^oC and is cooled by a water-cooled screw to below 90 °C. It is captured in a steel flask on a scale. Sampling of the kiln

feed is by grab samples from the belt every hour. Material captured in the radiation cooler and bagfilter is weighed and sampled (depending on the quantity and quality it could be discharged with the other CaS into the slaker). While one CaS flask fills the other one is cooled and discharged into the hopper feeding the slaking vessel.

2) Slaking or Slurring, Sulphide Stripping and Sulphur production

Slaking takes place when the cooled CaS is slurried with water. During slaking small quantities of sulphide (as $HS^-_{(aq)}$) are generated and therefore the slaking vessel is vented to the scrubbing circuit. Slaking takes place continuously by controlling the feedrate of CaS and water to the slaking vessel. CaS feed rate is set by adjusting the manual variable speed of the screw feeder from the hopper into the slaking vessel. As the slaking reaction is virtually instantaneous, the slaking vessel can be considered a CSTR (Continuous Stirred Tank Reactor).

After slaking, the next step is stripping of sulphide from the CaS. This is achieved by pumping the slurry into a jacketed reactor at 4 bar pressure and bubbling through.CO_2 from the kiln. The slurry is heated to 60 °C and H_2S is stripped off. The stripping reaction is controlled by controlling the pH in the stripping vessel through the feedrate of CO_2 to the vessel. Two stripping vessels are used and they are arranged such that the feed of CO_2 can be done in parallel or counter-currently. The process is followed by assaying the slurry from the second vessel. H_2S from the stripping vessel is compressed by a blower and fed to the PIPco reactor where conversion to sulphur takes place.

The unique feature of the PIPco process is that the reaction takes place in a buffered citric acid solution (pH 4-6) at 125 °C and 3-4 bar pressure. These conditions are chosen because sulphur is a liquid at that temperature and the higher pressure reduces evaporation of water.

Approximately 1/3 of the sulphur formed in the PIPco reactor is combusted with excess air at 1000 °C to SO_2. The SO_2 gas is cooled to below 50 °C in a

water/gas cooler. The cooled SO_2 is absorbed into citric acid to about 120 g/ℓ SO_2 in an absorption column. Vent gases from the absorption column are scrubbed in a milk of lime scrubber to absorb any residual SO_2 gas. The rich citrate solution is mixed with the H_2S gas and heated to 125 °C and then pumped at 3-4 bar pressure into the PIPco reactor. In the PIPco reactor the Claus reaction takes place which converts hydrogen sulphide and sulphur dioxide into elemental sulphur and water.

Liquid sulphur is periodically tapped off from the bottom of the reactor and granulated in water. It is scraped from the granulation tank and air dried and weighed. Vent gases leave the top of the reactor and lean citrate solution is cooled to below 50 °C and loaded again with SO_2 to repeat the process. The vent gases are scrubbed in a small milk of lime scrubber to capture any H_2S and SO_2 present as insoluble calcium compounds. A small percerntage of the combusted sulphur enters the circuit as SO_3 and will accumulate in the cooled citrate tank as potassium sulphate. It is removed from time to time and dried and assayed to complete the sulphur balance.